IL-6 SECRETION BY ASTROCYTES IN FRAGILE X MICE

ACTIVATION OF TLR4 BY TENASCIN C THROUGH THE INDUCTION OF INTERLEUKIN-6 IN THE FRAGILE X MOUSE MODEL

By: VICTORIA KRASOVSKA, B.Sc.

A Thesis Submitted to the School of Graduate Studies

In Partial Fulfilment of the Requirements

For the Degree

Master of Science

MASTER OF SCIENCE (2018) McMaster University (Science—Medical Science) Hamilton, Ontario

TITLE: Activation of TLR4 by Tenascin C through the induction of Interleukin-6 in the Fragile X mouse model

AUTHOR: Victoria Krasovska, B.Sc. (McMaster University)

SUPERVISOR: Dr. Laurie C. Doering

NUMBER OF PAGES: 93

LAY ABSTRACT

Autism spectrum disorders (ASDs) are neurodevelopmental disorders which arise from genetic and environmental factors. In the brain, a type of cell called the astrocyte is responsible for proper brain growth and development. Astrocytes release factors that promote inflammation, causing disruption of brain functions that control learning, memory and behaviour. Such factors released by astrocytes are capable of binding to their receptors, in turn impacting downstream targets, which have physiological effects.

This research used various biological and genetic techniques to determine if the mechanism of an astrocyte-specific factor called Tenascin C (TNC) is impaired in the Fragile X mouse model. In a normal astrocyte, TNC with its binding partner is able to release molecules responsible for inflammation. Such molecules have been shown to increase the number synapses, where neurons and astrocytes exchange information, to control brain function.

This proposed research would be the first to determine a role for TNC in ASDs. By assessing the cellular mechanisms involved between TNC and its binding partner, a novel therapeutic option could be made available in ASDs.

ABSTRACT

Fragile X syndrome (FXS) is identified by abnormal dendrite morphology and altered synaptic protein expression. Astrocyte secreted factors such as Tenascin C (TNC), may contribute to the synaptic changes, including maturation of the synapse. TNC is a known endogenous ligand of toll-like receptor 4 (TLR4) that has been shown to induce the expression of pro-inflammatory cytokines such as interleukin-6 (IL-6). At the molecular level, elevated IL-6 promotes excitatory synapse formation and increases dendrite spine length. With these molecular changes linked to the phenotype of FXS, we examined the expression and the mechanism of the endogenous TLR4 activator TNC, and its downstream target IL-6 in astrocytes from the *FMR1* KO mouse model. Secreted TNC and IL-6 were significantly increased in *FMR1* KO astrocytes. Exogenous TNC and lipopolysaccharide (LPS) stimulation of TLR4 induced secreted IL-6, whereas the antagonist of TLR4 (LPS-RS) had an opposing effect. Cortical protein expression of TNC and IL-6 were also significantly elevated in the postnatal *FMR1* KO mouse. These results identify TNC as an endogenous ligand of TLR4, capable of effecting IL-6 secretion by astrocytes. In addition, there was an increase in the number of VGLUT1/PSD95 positive synaptic puncta of both WT and *FMR1* KO neurons when plated with astrocyte conditioned media from *FMR1* KO astrocytes, compared to those plated with media from wild type astrocytes. By assessing the cellular mechanisms involved, a novel therapeutic option could be made available to target abnormalities of synaptic function seen in FXS.

ACKNOWLEDGEMENTS

This thesis represents a two-year process of research and experimentation. The endless hours of research required for this project would not have been accomplished without a network of support present inside and outside of the lab. Firstly, I would like to thank my supervisor, Dr. Laurie C. Doering. Without the resources present in his laboratory, and his constant support, this research would not have been a success. I would like to extend my deepest gratitude. The guidance and support I have received from my lab mates, Kathryn Reynolds, Angela Scott, Shivraj Jhala, Amanda Poxon and Chloe Wong, has been endless. Working with such dedicated and optimistic scientists made it a pleasure coming into lab each day. Speaking both personally an academically, I am very grateful.

I would like to extent my appreciation, to the members of my committee, Dr. Jane Foster and Dr. Ram Mishra. The feedback, criticism and guidance have tremendously benefited this research.

Lastly, I would like to extend my love and gratitude to my family. To my parents, I could have not done this without your endless love and support. Even under tremendous stress, you have always been there for me and supported all my decisions.

Additionally, to my partner and his family, I have benefitted from much support and feedback that you have provided. I am extremely grateful to be surrounded by such wonderful people.

TABLE OF CONTENTS

LIST OF FIGURES

LIST OF ABBREVIATIONS

ASD, autism spectrum disorders
TNC, Tenascin C
TLR, toll like receptor
TLR4, toll-like receptor 4
IL-6, interleukin-6
FXS, Fragile X Syndrome
FMR1, Fragile X Mental Retardation 1
FMRP, Fragile X Mental Retardation Protein
mGluR, metabotropic glutamate receptor
LTD, long-term depression
ECM, extracellular matrix
mGluR5, metabotropic glutamate receptor 5
TA, Tenascin Assembly
EGF-L, epidermal growth factor like domain
FN3, fibronectin type 3 like repeats
FBG, fibrinogen-like globe domain
TNF-α, tumour necrosis factor alpha
IL-1β, interleukin-1beta
BBB, blood brain barrier
PAMP, pathogen associated molecular patterns
DAMP, damage associated molecular patterns
LPS, lipopolysaccharides
CD14, cluster of differentiation 14
MD-2, myeloid differentiation factor 2
MyD88, myeloid differentiation primary response protein 88
Erk1/2, extracellular signal related kinase ½
JAK, Janus kinase
STAT, signal transducer and activator of transcription
PI3, phosphatidyl inositol-3 kinase
IRS, insulin receptor substrate
GSK3, Glycogen-synthase-kinase 3
NMM, neural maintenance media
BSA, bovine serum albumin
VGLUT1, Vesicular Glutamate Transporter 1 antibody
PSD95, post synaptic density protein 95
GFAP, glial fibrillary acidic protein
MWCO, molecular weight cut-off
ACM, astrocyte conditioned media
DAPI, 4', 6-diamidino- 2-Phenylindole
MAPK, mitogen-activated protein kinases
NFκB, nuclear factor κB

CHAPTER ONE

GENERAL INTRODUCTION

1.1 Fragile X Syndrome

Fragile X Syndrome (FXS) is the most common inherited form of autism which affects 1:4000 males and 1:8000 females (Hatton et al. 1998; Duy and Budimirovic 2017; Jin and Warren 2000). A multitude of symptoms occur in FXS ranging from mild to severe behavioural deficiencies such as cognitive impairment, hyperactivity, anxiety, autistic-like behaviours, susceptibility to seizures and motor disorders (Contractor, Klyachko, and Portera-Cailliau 2015; Hunsaker 2012). The defects in individuals with FXS are attributed to the mutation in the Fragile X Mental Retardation 1 (*FMR1*) gene resulting from the expansion of the CGG untranslated region of the X chromosome (Jin and Warren 2000). This expansion leads to the hypermethylation and silencing of the *FMR1* gene, preventing the synthesis of the Fragile X Mental Retardation Protein (FMRP) (Jin and Warren 2000).

1.2 The *FMR1* KO mouse model of Fragile X Syndrome

The *FMR1* knockout mouse model of FXS was developed in 1994 (FVB.129p2(B6)-*Fmr1*), and has been shown to share similar behavioural characteristics as those seen in individuals with FXS such as susceptibility to seizures, hyperactivity and learning impairments (Shelley Jacobs and Doering 2010). The development and use of this mouse model has lead to tremendous advancements in cellular and molecular mechanisms in the pathology of FXS (Shelley Jacobs and Doering 2010; Pfeiffer and Huber 2009; Gatto and Broadie 2010). However, more research is required to fully

understand the cellular mechanisms in the animal model, which can be transferred to the human model in order to understand the FXS pathology.

1.2 FMRP

FMRP is an mRNA binding protein which regulates the translation, and transport of mRNA in the brain, with the highest levels seen in hippocampal and cerebellar neurons (Pacey et al. 2015). The lack of FMRP in FXS has been associated with abnormal synapse formation, synapse number and structure (Yang et al. 2016; Pfeiffer and Huber 2009). In neurons, FMRP is known to regulate synaptic plasticity; in particular metabotropic glutamate receptor (mGluR) mediated long-term depression (LTD) (Contractor, Klyachko, and Portera-Cailliau 2015). Under normal conditions FMRP is expressed in neurons (Arsenault et al. 2016), astrocytes and oligodendrocytes where it influences the synaptic environment to bind, transport and translocate mRNA (H. Wang et al. 2004) .

1.4 Astrocytes and the synapse

Studies from recent years have determined that astrocytes perform a wider range of functions than initially thought, such as modulating neurovascular blood flow, maintaining homeostasis and regulating the synaptic environment (Molofsk et al. 2012; Faissner et al. 2010). The synapse is a central relay system consisting of a pre-synaptic and post-synaptic neuron, separated by a synaptic cleft (Faissner et al. 2010). Accordingly, neuron- and glia-derived cytokines, metabolites and neurotrophins have been found to influence the synaptic environment in addition to neuronal growth and

plasticity. Interestingly, the maintenance of plasticity in the CNS has been shown to correspond with extracellular matrix (ECM) glycoproteins, that are otherwise found to be down-regulated, namely such as Tenascin C (Faissner et al. 2010). Additionally, co-culture experiments have been done to strengthen this concept and clearly indicate the impact of astrocyte secreted factors on the maturation and functional activation of synapses (S. Jacobs, Cheng, and Doering 2016).

1.5 Astrocytes and Fragile X Syndrome

A growing body of research indicates a crucial role of astrocytes in synapse development, in particular the role of synapse structure, function and plasticity (Molofsk et al. 2012; Willis and Crocker 2016). Overall, the synaptic function remains as the prominent link to a number of neurodevelopmental disorders such as FXS. There is a tremendous amount of evidence that suggests a role for FMRP in synapse development, elimination and plasticity (Contractor, Klyachko, and Portera-Cailliau 2015). FMRP has been implicated in synaptic plasticity on the basis of dendritic spine abnormalities and exaggerated long-term depression (LTD) displayed by *FMR1* KO mice (Cheng, Lau, and Doering 2016; Arsenault et al. 2016; H. Wang et al. 2004). Additionally, FMRP has been shown to function as a translational repressor of specific mRNAs, resulting in downregulation of metabotropic glutamate receptor 5 (mGluR5) activity through a negative feedback loop (Yang et al. 2016). Most importantly, co-culture experiments were able to display a rescue of synaptic morphology and protein expression when *FMR1* KO neurons were cultured with WT astrocytes (Cheng, Sourial, and Doering 2012). This

solidifies the importance of astrocytes in the abnormal dendritic morphology and dysregulated synaptic development seen in FXS.

1.6 Astrocyte-secreted factor Tenascin C

Astrocytes secrete a number of factors which determine synapse development, neuronal activation and plasticity (Jones and Bouvier 2014). TNC is one of the secreted extra-cellular matrix glycoproteins which is part of a family consisting of four homologs of Tenascin R, Tenascin X and Tenascin W (Giblin and Midwood 2015). TNC consists of 4 distinct domains giving it ability to interact with 25 different molecules consisting of matrix proteins, soluble factors and cell surface proteins (Giblin and Midwood 2015). Each TNC monomer contains a Tenascin Assembly (TA) domain, 14.5 epidermal growth factor like (EGF-L) repeats, fibronectin type 3 (FN3) like repeats, followed by a fibrinogen-like globe (FBG) domain (Giblin and Midwood 2015). Each monomer of TNC forms trimers via coil interaction by which they are then covalently bound to make a hexabrachion (Giblin and Midwood 2015). Typically, the FN3 domain consists of 8 repeats, although due to alternative splicing, different numbers of FN3 domains can occur. TNC is transiently expressed by neural and glial cells during development and plays a crucial role of extracellular matrix re-modeling during tissue repair (Jones and Bouvier 2014). The overall expression of TNC decreases with increasing age, peaking during embryonic development and shortly after birth (Giblin and Midwood 2015). During adulthood, TNC expression should be present in low levels in healthy tissue, while in the diseased or injured state expression would peak (Giblin and Midwood 2015).

As TNC expression increases, it begins to act as both as a repulsive and permissive substrate for neuronal and astrocytic growth (Jones and Bouvier 2014) . TNC is also known to influence astrocyte proliferation and process elongation through autocrine/paracrine mechanisms (Jones and Bouvier 2014).

In a diseased brain, TNC has been shown to be up-regulated at the sites of injury, in correlation with astrocyte reactivity and glial scar formation. Stab wounds in the cerebellar and cortical structures have been shown to enhance production of TNC in GFAP positive astrocyte in proximity to the site of injury (Jones and Bouvier 2014). In stab wound assays, astrocytes in culture also exhibited an increase of TNC (Jones and Bouvier 2014). Studies with TNC null mice revealed that GFAP expression was significantly weaker one week after the stab wound, which is usually correlated with the severity of reactivity (Jones and Bouvier 2014) . The same study has also confirmed increased levels of pro-inflammatory cytokines such as tumour necrosis factor alpha (TNF alpha), IL-6 and IL-1β (Jones and Bouvier 2014) . These results suggest that TNC may influence the blood-brain barrier (BBB) repair and regulation of inflammatory cytokines.

TNC has been found to be up-regulated in a number of neurodegenerative diseases such as Alzheimer's Disease (AD) and Down syndrome (Meiners et al. 1999; Giblin and Midwood 2015). Recently, TNC has been reported to be utilized as a plasma biomarker for AD, Down syndrome and other mild cognitive impairment patients (Jones and

Bouvier 2014). In particular, loss of TNC in the CRND8 AD-like mouse model has enhanced the production of anti-inflammatory cytokine and reduced pro-inflammatory cytokines which is in contrast with the inflammation seen in terms of physical activity, thus TNC may act as a promoter or inhibitor based on the type of insult (Jones and Bouvier 2014) . Particularly, pro-inflammatory cytokine production via the activation of TLR4 in non-neuronal cells has been exhibited (Midwood et al. 2009; Maqbool et al. 2016). In support of this, TLR4 is expressed at the surface of astrocytes and microglia and has been found to induce inflammation in neurodegenerative disease (Trotta et al. 2014).

1.7 Tenascin C Receptor: Toll-like receptor 4

Toll-like receptors (TLRs) are key players in innate immunity, which act by recognizing pathogen and damage associated molecular patterns (PAMPs and DAMPs) mediating host defense against infection and injury (Midwood et al. 2009; Henneberger and Steinhäuser 2016). PAMPs are essential structures required for the surveillance of pathogens, with the classic example of lipopolysaccharides (LPS) (Gorina et al. 2011). LPS binding to TLR4 is dependent on cluster of differentiation 14 (CD14) and myeloid differentiation factor 2 (MD-2), which triggers myeloid differentiation primary response protein 88 (MyD88) dependent and independent pathways (Midwood et al. 2009).

DAMPs are endogenous pro-inflammatory molecules generated during injury and include extracellular matrix proteins such as TNC (Midwood et al. 2009). During the innate and adaptive immune responses, there is an induction of pro-inflammatory

cytokines such as IL-6 and matrix metalloproteinase (Midwood et al. 2009). The FBG domain of Tenascin C has been found to promote cytokine production, stimulating TNF-α, IL-6 and IL-8 in the synovial fibroblast (Midwood et al. 2009). Unlike TLR4 activation by LPS, neither CD14 nor MD-2 is required for TLR4 activation by TNC (Midwood et al. 2009).

In the CNS, TLR4 has been found to be highly expressed in microglia, as well as neurons, astrocytes, and oligodendrocytes (Garcia Bueno et al. 2016). Neurons and astrocytes are capable of detecting DAMPs and are able to initiate CNS inflammation through a TLR4 dependent mechanism (Garcia Bueno et al. 2016) . Peripheral TLR4 activation has been shown to disrupt gap junctions among astrocytes causing mesial temporal lobe epilepsy (Shen et al. 2016). LPS dependent activation of TLR4 in astrocytes increased astrocytic extracellular signal related kinase (Erk1/2) and phospho-Erk1/2 levels in a MyD88 dependent manner which enhanced excitatory synaptogenesis in the hippocampus (Shen et al. 2016).

1.8 Downstream target of TLR4/Tenascin C: Interleukin-6

Interleukin-6 (IL-6) is a cytokine in the form of a four helix bundle which binds to class I receptors that require additional receptor proteins: gp130, βc or γc (Erta, Quintana, and Hidalgo 2012). The hexamer formed consists of two IL-6, two IL-6R and two gp130 that can activate tyrosine kinases such as Janus kinase (JAK) which then activates a number of proteins including the signal transducer and activator of transcription (STAT)

family of transcription factors, or the RAS-RAF-MAPK pathway, phosphatidyl inositol-3 kinase (PI3), or insulin receptor substrate (IRS) (Erta, Quintana, and Hidalgo 2012).

IL-6 expression in the brain was first demonstrated in the astrocytoma and glioma lines which expressed IL-6 when stimulated with IL-1β (Erta, Quintana, and Hidalgo 2012). These finding deduced that IL-6 and IL-6R is expressed in glial and neuronal cells throughout the brain (Erta, Quintana, and Hidalgo 2012). IL-6 plays a tremendous role in adults neurogenesis, in particular creating new neurons and glial cells from neural stem cells, who's up-regulation is implicated in a variety of neuropathological conditions (Erta, Quintana, and Hidalgo 2012). Increased IL-6 in the brain has been associated with severe cognitive impairments, behavioural deficits and neuronal loss (Beurel et al. 2009) . In particular, elevated brain, plasma, peripheral blood cells and lymphoblast IL-6 levels have been noted, which suggests that reactive glia or maternal immune activation could be responsible for IL-6 dysregulation (H. Wei, Alberts, and Li 2013).

1.9 STAT3 and GSK3 in the FXS mouse model

Glycogen-synthase-kinase 3 (GSK3) has recently been identified as a crucial regulator of the innate inflammatory response which strongly promotes toll-like receptor production of cytokines (Beurel et al. 2009) . Interestingly, in mouse models of FXS, GSK3 activity has been found to be elevated, as GSK3β translation has been found to be modulated by FMRP (Beurel et al. 2009). STAT3 in conjunction with GSK3 has been found to act in a pro-inflammatory way in the CNS, which greatly induced IL-6

production in glial cells (Beurel et al. 2009). In addition, it has been found that IL-6 induces the phosphorylation of JAK2 and activation of STAT3, also resulting in a release of pro-inflammatory cytokines IL-1β and TNF-α (Beurel et al. 2009). Thus, it is important to determine the role of STAT3 in FXS, as the role of GSK3 has been previously explored.

CHAPTER TWO

RATIONALE, CENTRAL HYPOTHESIS AND RESEARCH AIMS

2.1 Rationale for the study

The role of astrocyte secreted factors in neurodevelopmental disorders such as FXS have only recently been under investigation. In particularly, neuroimmunology has been recently studied in hope of finding more information for the role of the immune system within the CNS. One of the cytokines responsible for a multitude of functional aspects in neurodevelopmental disorders is IL-6. Thus, by exploring this cytokine, in addition to the TNC-TLR4-IL-6 axis, provides the scientific community with a potential novel pathway that is dysfunctional in FXS.

2.2 Central Hypothesis

Dysfunctional IL-6 signalling through the Tenascin C-TLR4-IL-6 axis in the FXS mouse model may lead to improper synapse development and function.

2.3 Research Aims

2.3.1 Determine postnatal expression of astrocyte secreted TNC, TLR4 and IL-6 *in vitro*.

Tenascin C and IL-6 have been both implicated in synaptic development. However, these two proteins have been found to be related though the activation of TLR4. Thus, we compared the expression of TNC, TLR4 and IL-6 in the developing cortex of WT and *FMR1* KO mice aged P1, P7, P14 and P21.

2.3.2 Observe cell associated and secreted TNC and IL-6 in primary astrocyte cultures in the naive state, in addition to LPS, exogenous TNC, LPS-RS and TAK242 treated cells.

Both TNC and IL-6 are astrocyte secreted factors, however neither TNC nor IL-6 have been studied in FXS. Additionally, treating astrocyte cultures with agonists of TLR4; LPS and TNC, as well as antagonist of TLR4; LPS-RS and TAK242 provide us with greater clues as to what impacts the production and secretion of IL-6.

2.3.3 Analyze the number of excitatory synaptic connections in WT and *FMR1* KO neuronal cultures supplement with astrocyte conditioned media from WT and *FMR1* KO astrocytes.

Astrocytes are developmentally important in the formation and maturation of synaptic connections. IL-6 has been implicated in increasing the number of excitatory synapses and decreasing the number of inhibitory synapses. For the aspect of FXS, it was interesting to determine how astrocyte secreted factors such as IL-6 impact excitatory synapse formation.

2.3.4 Determine the role of STAT3 and IL-6 secretion by astrocytes.

STAT3 has been recently identified to be highly dependent on GSK3, which is a key metabolic regulator. Additionally, GSK3 has been determined to be hyperactive in the FXS mouse brain, however, with the addition of lithium, this activation was restored to normal. Thus, due to the dependency on GSK3, it was important to determine whether a

STAT3 knockdown with siRNA had an impact on IL-6 secretion in the FXS mouse model.

CHAPTER THREE

EXPERIMENTAL DESIGN

3.1 Animals

WT and *FMR1* KO mice (FVB.129P2[B6]-Fmr1 tm1Cgr) were housed and bred in the McMaster University Central Animal Facility. All experiments and animal-handling procedures followed the guidelines set by the Canadian Council on Animal Care and were approved by the McMaster Animal Research Ethics Board (AUP 13-12-49).

3.2 Cortical Tissue Isolation for Western Blotting

Wild-type (WT) and knockout (*FMR1* KO) mice were decapitated and whole brains were extracted at P1 (6 males and 2 females), P7 (5 males and 3 females), P14 (6 males and 2 females) and P21 (8 males and 0 females) into ice cold, sterile phosphate-buffered saline (PBS, 0.01 M). Cortical samples were dissected and were immediately flash-frozen in isopentane and stored at -80 °C. Samples were mechanically homogenized on ice in lysis buffer (150 mM NaCl, 1% NP40, 0.5% Deoxycholic Acid, 1% SDS, 50 mM Tris, Roche ULTRA protease inhibitor tablet, Roche PhoSTOP phosphatase inhibitor tablet). Homogenized tissue samples were left on ice for 1 h and centrifuged at 16,000 rpm for 15 mins at 4 °C. The supernatant was collected and the protein concentration of each sample was determined by a DC protein assay (Bio-Rad, Missasauga, ON, CA). Samples were aliquoted and stored at -80 °C.

3.3 Primary Cortical Astrocyte Culture

Primary cultures of astrocytes were isolated from *FMR1* knockout (*FMR1* KO) and wild-type (WT) mice as described by Jacobs & Doering (2009). Cortical astrocytes were

isolated from WT and *FMR1* KO mice at P1 or P2 and grown in a T75 culture flask in minimum essential media (Invitrogen, Carlsbad, CA, USA), supplemented with 30% glucose and 10% horse serum (Invitrogen). Culture were maintained for approximately 1 week or until 70% confluent at 37°C and 5% CO_2. Cells were then removed from the T75 flask with the addition of Trypsin-EDTA 0.05% (Invitrogen) and re-plated on 24 well plates with coverslips for immunocytochemistry experiments or on to 6 well plated for collection of astrocyte conditioned media. The 24 well plate contained coverslips coated with Poly-L-Lysine (Sigma-Aldrich, St. Louis, MO, USA; 1mg/mL) and laminin (Invitrogen; 0.1mg/mL), and seeded with 5000 cells per well. Cells were maintained for 3 days *in vitro* for subsequent immunocytochemistry. The 6 well plates were also coated with Poly-L-Lysine (Sigma-Aldrich, St. Louis, MO, USA; 1mg/mL) and laminin (Invitrogen; 0.1mg/mL), and seeded at a density of 100,000 cells per well. Cells were maintained for 3 to 5 days *in vitro* for analysis of ACM and cell collection via Western Blotting.

3.4 Western Blotting

Cortical samples containing 30 ug (homogenized whole tissue) of protein were combined with sample buffer (1X; 5% Beta-Mecaptoethanol+ Laemmli Sample Buffer, Bio-Rad). Samples were boiled at 95 °C for 5 mins, briefly centrifuged and loaded onto 4-15 % precast polyacrylamide stain-free gel (Bio-Rad). Proteins were separated via electrophoresis at 135V, activated with UV light (302nm) for visualization of total protein (1 min) and transferred onto polyvinylidene difluoride (PVDF) membrane (Bio-Rad)

using the Trans-Blot Turbo Transfer System (Bio-Rad). The membranes were then imaged for total loaded protein using a ChemiDoc Imaging System (Bio-Rad, Mississauga, ON, CA), after which they were blocked for 1 h in a blocking solution (5% non-fat milk solution in Tris-buffered saline solution with Tween-20 (TBS-T). Each membrane was then incubated overnight at 4 °C in TBS-T containing anti-rat Tenascin C antibody (host rabbit; 1:250; MAB2138; R&D Systems), anti-mouse TLR4 antibody (host rabbit; 1:250; 76B357.1; abcam), anti-mouse IL-6 antibody (host rabbit; 1:500; ab9324; abcam), anti-rabbit IL-6R antibody (host rabbit; 1:500; 128008; abcam), anti-mouse STAT3 antibody (host mouse; 1:1000; 9139; Cell Signaling) and anti-rabbit phosphor-STAT3 (Tyr 705) (host rabbit; 1:1000; 9131; Cell Signaling). These antibodies recognize bands at 250 kDa corresponding to Tenascin C (Fig. 1B), 73 kDa corresponding to TLR4 (Fig. 2B), 50 kDa corresponding to IL-6 (Fig. 3B), 60 kDa corresponding to IL-6R (Fig. 9), 86 kDa corresponding to STAT3 and phos-STAT3 (Fig. 10). Following incubation, the membranes were washed 3 x 10 mins in TBS-T and then incubated in TBS-T containing horseradish peroxidase conjugated secondary antibody against rat (1:10,000; ab97057; abcam), mouse (1:5000; NA931V; GE Healthcare Life Sciences) or rabbit (1:2500; NA934; GE Healthcare Life Sciences) for 1 h at room temperature. Following the incubation period, membranes were then washed 3 x 10 mins in TBS-T and developed using enhanced chemiluminescence developer solutions (Bio-Rad). Membranes were scanned using a ChemiDoc Imaging System (Bio-Rad, Mississauga, ON, CA). Densitometry measurements were conducted using Image Lab Software 5.2 (Bio-Rad). Each band corresponding to either TNC (~250 kDa), TLR4 (~73

kDa), IL-6 (~50 kDa), IL-6R (~60 kDa), STAT3 (~86 kDa) or phos-STAT3 (~86 kDa) was first normalized to total protein within the same lane and then to a cross gel control. These values were then expressed as a relative percentage of the average densitometry value obtained from the age-matched WT samples.

3.5 Cortical Neurons maintained with Cortical Astrocyte Conditioned Media

Cortical astrocytes were isolated from WT and *FMR1* KO mice at P1 or P2 and grown in a T75 culture flask in minimum essential media (Invitrogen, Carlsbad, CA, USA), supplemented with 30% glucose and 10% horse serum (Invitrogen). Culture were maintained until 70% confluent at 37°C and 5% CO_2. After confluency has been reached, the media was switched to neural maintenance media (NMM) (StemCell Technologies), and supplemented with SM1 (StemCell Technologies), GlutaMAX (Gibco) and 2mg/ml L-Glutamic Acid (Sigma). The media was conditioned for 3 days before it could be used to supplement neuronal cultures. WT and *FMR1* KO neurons were plated on coverslips in a 24-well plate with Poly-L-Lysine (Sigma-Aldrich, St. Louis, MO, USA; 1mg/mL) and laminin (Invitrogen; 0.1mg/mL), and seeded at a density of 10,000 cells per well in the conditioned NMM. Neuronal cultures were maintained for 12 days at 37°C and 5% CO_2 and then processed for immunocytochemical analysis.

3.6 Immunocytochemistry

Immunocytochemistry experiments were carried out with primary cortical astrocyte cultures following a protocol previously described by Cheng et al. (2016). The astrocytes

were fixed with 4% PFA for 20 mins at room temperature. The cells were washed three times with PBS and permeabilized with 0.1% Triton-X-100. Non-specific binding was blocked with 1.0% Bovine Serum Albumin (BSA) for 30 mins at room temperature. Primary antibodies were prepared in PBS and applied to the coverslips for 24 h. The following primary antibodies were used: anti-rat Tenascin C antibody (host rabbit; 1:50; MAB2138; R&D Systems), anti-mouse TLR4 antibody (host rabbit; 1:500; 76B357.1; abcam), anti-mouse IL-6 antibody (host rabbit; 1:1000; ab9324; abcam), anti-rabbit IL-6R antibody (host rabbit; 1:500; 128008; abcam), anti-mouse STAT3 antibody (host mouse; 1:1500; 9139; Cell Signaling) and anti-rabbit phosphor-STAT3 (Tyr 705) (host rabbit; 1:500; 9131; Cell Signaling) and anti-chicken GFAP (1:2000; CH22102; Neuromics, Minneapolis, MN, USA). The second day, the coverslips were washed three times with PBS, following incubation with the secondary antibody for 3 h at room temperature. These included goat anti-rat Alexa Fluor 488 (1:200; ab150157; abcam), donkey anti-mouse Alexa Fluor 594 (1:1000; A-21203; Invitrogen), donkey anti-rabbit Alexa Fluor 488 (1:200; A-11008; Invitrogen), donkey anti-rabbit Alexa Fluor 698 (1:200; A-10042; Invitrohen), rabbit anti-chicken TRITC (1:100; 303-025-003; Jackson) and donkey anti-chicken FITC (1:100; 703-095-155; Jackson). Lastly, the coverslips were washed three times with water and PBS, following mounting with ProLong Gold Antifade Mountant with 4', 6-diamidino- 2-phenylindole (Life Technologies, Carlsbad, CA, USA). Three independent (n=3) cultures and a total of 27 cells were examined per genotype. Visual imaging was acquired using a Zeiss Axioskop 2 epifluoerescence microscope and Axiovision (v4.6) image acquisition software.

In addition, neuronal cultures supplemented with conditioned NMM, were processed in a similar manner to determine the co-localized VGLUT1 pre-synaptic and PSD95 post-synaptic puncta. The following primary antibodies were used: guinea pig anti-Vesicular Glutamate Transporter 1 antibody (VGLUT1; 1:200; AB5905; Millipore) and mouse anti-post synaptic density protein 95 (PSD95; 1:100; MAB1596; Millipore). The corresponding secondary antibodies were used: donkey anti-mouse Alexa Fluor 594 (1:1000; A-21203; Invitrogen) and donkey anti-guinea pig FITC (1:200, 706-095-148, Jackson ImmunoResearch). Sixteen independent neuronal cultures (n=4/condition) supplemented with conditioned NMM were examined. Ten neurons per condition were examined from 9 wells per n, resulting in synapse counts averaged from 40 neurons.

3.7 Measurements of Tenascin C and IL-6 expression and secretion

TNC and IL-6 levels were determined in astrocyte cultures and in astrocyte conditioned media (ACM). Confluent astrocyte cultures were incubated with 0.05 % Trypsin-EDTA for 5 mins at 37°C. Once cells were fully lifted, MEM media supplemented with serum was added to prevent further digestion. The samples were then centrifuged at 250xg for 5 mins at RT. The cells were then lysed with lysis buffer (150 mM NaCl, 1% NP40, 0.5% Deoxycholic Acid, 1% SDS, 50 mM Tris, Roche ULTRA protease inhibitor tablet, Roche PhoSTOP phosphatase inhibitor tablet). The lysates were collected in Eppendorf tubes and centrifuged at 15,000 rpm for 15 mins at 4°C. The supernatant was stored at −80 °C until further protein quantification to determine the cell associated concentrations.

Aliquots of ACM from the same culture were processed to determine the secreted (extracellular) TNC and IL-6 levels. In preparation for conditioning, ACM was harvested for 3 days with the MEM media replaced with serum free minimum-essential media on the third day, after which the sample was collected and concentrated. The media was filtered using a 0.22μm syringe filter for the removal of cellular debris and concentrated using Vivaspin 20 (GE Healthcare) through a 50 kDa molecular weight cut-off (MWCO) for TNC or Vivaspin 6 (GE Healthcare) through a 10 kDa MWCO for IL-6. ACM was stored at −80 °C until further protein quantification with Western Blotting.

3.8 Cortical Astrocyte Drug Treatments

To assess TLR4 activation, WT and *FMR1* KO cortical astrocyte cultures were treated with exogenous TNC, in addition to the known TLR4 agonist (LPS) to test IL-6 induction. Additionally, TLR4 antagonist treatments with LPS-RS and TAK242 were performed to examine for a decrease in cytokine expression. The astrocytes were grown for 3 to 5 days *in vitro* in serum-free minimum essential media (Invitrogen, Carlsbad, CA, USA) supplemented with 30% glucose, achieving 70% confluency. At 3 h, 6 h and 24 h prior to cell and ACM collections, astrocytes were treated with exogenous chicken Tenascin C (10 ug/mL; CC118, Millipore), LPS (10 ug/mL; Sigma-Aldrich), LPS-RS (10 ug/mL; Sigma-Aldrich) and TAK242 (5ug/mL; 614316, Millipore). The cells were trypsinized and collected as previously discussed. The ACM was filtered using a 0.22μm syringe and concentrated through a 10 kDa MWCO using Vivaspin 6 (GE Healthcare). The cell associated and secreted IL-6 protein levels were quantified using Western

Blotting and secreted IL-6 treated with LPS-RS and TAK242 treatments was quantified using ELISA (Invitrogen, KMC0061), according to manufacturers instructions.

3.9 Synaptic Puncta Analysis

Visual imaging was acquired using a Zeiss Axioskop 2 epifluorescence microscope and Axiovision (v4.6) image acquisition software. SynapCountJ, is a custom written plug-in for ImageJ (National Institutes of Health, Bethesda, MD, USA) used to identify co-localized puncta. Background was removed from both the red and green channels of each image using the ImageJ rolling ball background subtraction algorithm. Dendrite tracings were done using NeuronJ (an ImageJ plugin). The coordinates of these tracings were uploaded into SynapCountJ along with the corresponding red and green channel images. The number of co-localized puncta was measured for each tracing and normalized to the tracing length.

3.10 STAT3 knockdown in primary cortical astrocytes

For knockdown experiments, primary cortical astrocytes were seeded at a density of 100,000 cell/well, in 6 well plates. The cells were transfected using liposome-mediated transfection reagent Lipofectamine RNAiMAX (Invitrogen) with 50 nM siRNA according to instructions with STAT3 siRNA (Invitrogen) and silencer negative control (Invitrogen). For experimental treatments, cells were pre-treated with exogenous chicken Tenascin C (10 ug/mL; CC118, Millipore) for 3 hours prior to cell and ACM collection, as described previously. Mouse IL-6 was measured with an ELISA kit (Invitrogen,

KMC0061), according to the manufacturers instructions. Cell survival was determined by the use of a Dead Cell Dye from the BLOCK-iT Tranfection Optimization Kit (Invitrogen) according to manufacturers instructions (Fig.11B). Additionally, transfection efficacy was determined by transfecting primary cortical astrocytes with 25% STAT3 siRNA and 75% Fluorescent Oligo (Fig.11C). Subsequently, visualization was acquired using a Zeiss Axioskop 2 epifluorescence microscope.

3.11 Statistical Analysis

Statistical analysis was conducted using GraphPad Prism Software 7.0 (GraphPad Software Inc., San Diego, CA, USA). Unpaired, two-tailed t-tests were used to identify the differential expression of TNC, TLR4 and IL-6 between the WT and *FMR1* KO groups. Additionally, unpaired, two-tailed t-tests were used to identify differences of cell associated and secreted TNC and IL-6 expression of cultured cells and ACM. To determine statistical significance of the treatment groups and synaptic analysis, a two-way ANOVA, along with Tukey's multiple comparison tests were conducted. All results except for synaptic analysis are shown as mean ± SEM. Synaptic analysis are shown as a box and whiskers plot representing the mean with the interquartile range, with error bars representing the min and max values. Results deemed significant when probability values $P < 0.05$.

CHAPTER FOUR

RESULTS

In this study we investigated the developmental expression of TNC, TLR4 and IL-6 in cortical brain regions of WT and *FMR1* KO mice, aged P1, P7, P14 and P21. We hypothesized that the levels of astrocyte derived TNC are dysregulated in the *FMR1* KO mouse model, thus contributing to the elevated IL-6 levels, which may be responsible for the aberrant synaptic changes seen in FXS. While the expression of TLR4 remained consistent between the genotypes, treatments with LPS and exogenous TNC suggest that TLR4 is responsible for IL-6 secretion in astrocytes.

4.1 Tenascin C and IL-6 protein levels are altered in the cortex of *FMR1* KO mice.

TNC, TLR4 and IL-6 were all highly expressed in primary cortical astrocytes from the WT and *FMR1* KO P1 or P2 mice. All three targets showed similar distribution patterns between the groups following 3 days *in vitro* (n=3, 27 cells/group; Fig. 1A, 2A, 3A). To determine if there was differential expression of TNC, TLR4, and IL-6 in *FMR1* KO mice at P1, P7, P14 and P21, Western blotting experiments were conducted. There was a decrease of TNC expression between the WT and *FMR1* KO groups at P7 (86.03 ± 4.827, $P < 0.05$; n=8/group; Fig. 1B, D). At P14, TNC levels were increased in the *FMR1* KO group (121.4 ± 4.087, $P < 0.01$; n=8/group; Fig. 1B, E). Additionally, TNC levels were elevated in the *FMR1* KO group at P21 (116.1 ± 3.179, n=8; $P < 0.01$; n=8/group; Fig. 1B,F). Each n represented a biological replicate.

Since TNC is a known ligand of TLR4, we analyzed the cortical protein expression. Western blotting for TLR4 revealed no differences in expression between WT and *FMR1* KO groups at P1, P7, P14 or P21 (Fig. 2B-F).

Since TLR4 activation by TNC results in the synthesis of IL-6, we analyzed IL-6 cortical protein expression. These experiments revealed a difference in IL-6 protein expression between the WT and *FMR1* KO groups at P7, P14 and P21. At P7, the *FMR1* KO group showed higher IL-6 levels than the WT group (159.2 ± 24.01; $P < 0.05$; n=8/group; Fig. 3B, D). At P14, the *FMR1* KO group once again showed different IL-6 levels between the groups (116.4 ± 5.091, $P < 0.05$; n=8/group; Fig. 3B, E). There were also differences of IL-6 expression at P21 between the WT and *FMR1* KO groups (145.0 ± 11.46, $P < 0.001$; n=8/group; Fig. 3B, F).

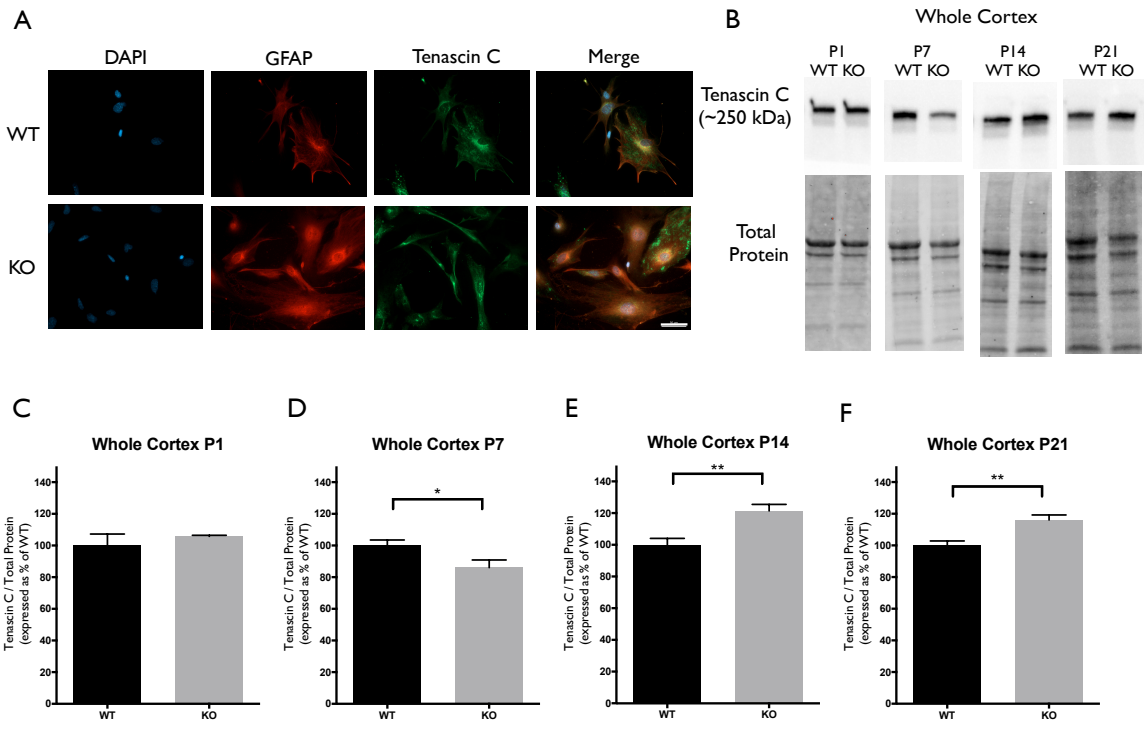
A
DAPI
GFAP
Tenascin C
Merge
WT
KO
B
Whole Cortex
P1 WT KO
P7 WT KO
P14 WT KO
P21 WT KO
Tenascin C (~250 kDa)
Total Protein
C
Whole Cortex P1
D
Whole Cortex P7
E
Whole Cortex P14
F
Whole Cortex P21
Tenascin C / Total Protein (expressed as % of WT)
WT
KO
*
**

Figure 1: Tenascin C expression is significantly altered at postnatal period P7-P21 in the cortex of *FMR1* KO mice. (A) Cultured cortical astrocytes co-labelled with anti-glial fibrillary acidic protein (GFAP; red), 4', 6-diamidino- 2-Phenylindole (DAPI; blue) and anti-tenascin C (green) after 3 days *in vitro*. Images were obtained using a 40x objective with a Zeiss Axioimager M2. Scale bars=50μm. **(B)** Western blots showing Tenascin C expression (~ 250 kDa) in cortical samples containing 30 μg of protein from P1 (6 males and 2 females), P7 (5 males and 3 females), P14 (6 males and 2 females) and P21 (8 males and 0 females) WT and *FMR1* KO mice. Corresponding total protein was used as a loading control. **(C-F)** Cortical expression of Tenascin C in WT (black; n=8) and *FMR1* KO (grey; n=8) mice at P1, P7, P14 and P21. Representative bands were normalized to the total protein and expressed as a percentage of the average Tenascin C in the WT group. Statistical differences denoted with a single asterisk, $P < 0.05$ and with a double asterisk, $P < 0.01$.

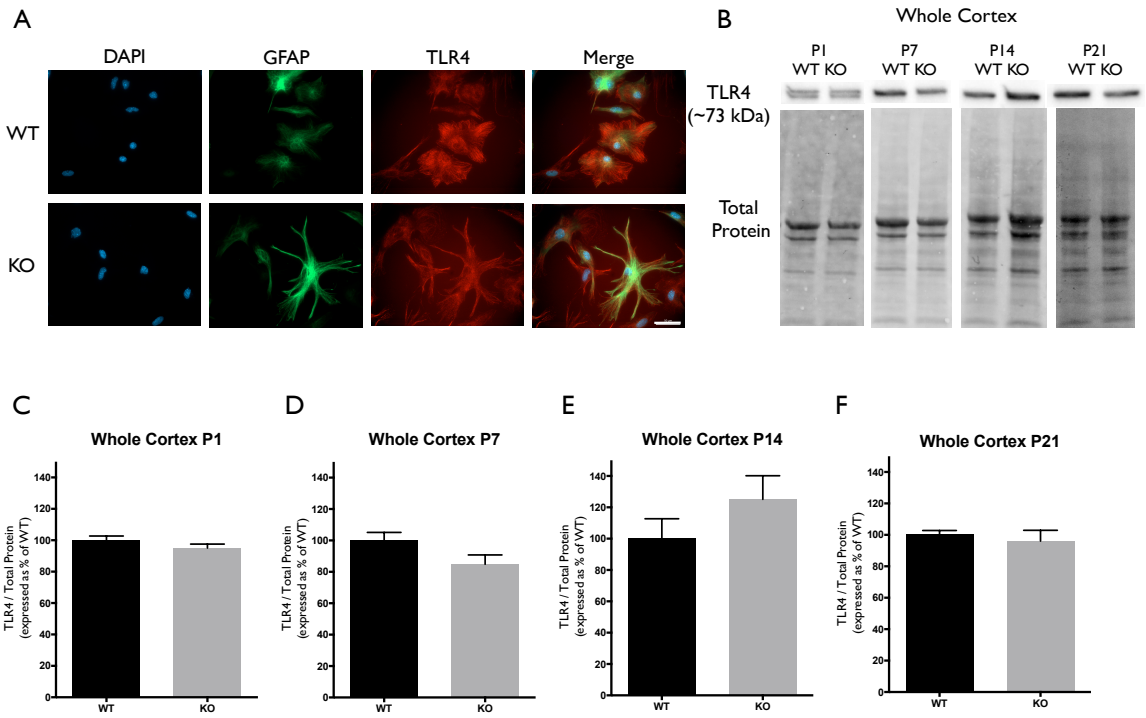
A
DAPI
GFAP
TLR4
Merge
WT
KO
B
Whole Cortex
P1 WT KO
P7 WT KO
P14 WT KO
P21 WT KO
TLR4 (~73 kDa)
Total Protein
C
Whole Cortex P1
D
Whole Cortex P7
E
Whole Cortex P14
F
Whole Cortex P21
TLR4 / Total Protein (expressed as % of WT)
WT
KO

Figure 2: TLR4 expression is not significantly altered in the cortex of *FMR1* KO mice. (A) Cultured cortical astrocytes co-labelled with anti-glial fibrillary acidic protein (GFAP; green), 4', 6-diamidino- 2-Phenylindole (DAPI; blue) and anti-TLR4 (red) after 3 days *in vitro*. Images were obtained using a 40x objective with a Zeiss Axioimager M2. Scale bars=50µm. **(B)** Western blots showing TLR4 expression (~ 73 kDa) in cortical samples containing 30 µg of protein from P1 (6 males and 2 females), P7 (5 males and 3 females), P14 (6 males and 2 females) and P21 (8 males and 0 females) WT and *FMR1* KO mice. Corresponding total protein was used as a loading control. **(C-F)** Cortical expression of TLR4 in WT (black; n=8) and *FMR1* KO (grey; n=8) mice at P1, P7, P14 and P21. Representative bands were normalized to the total protein and expressed as a percentage of the average TLR4 in the WT group.

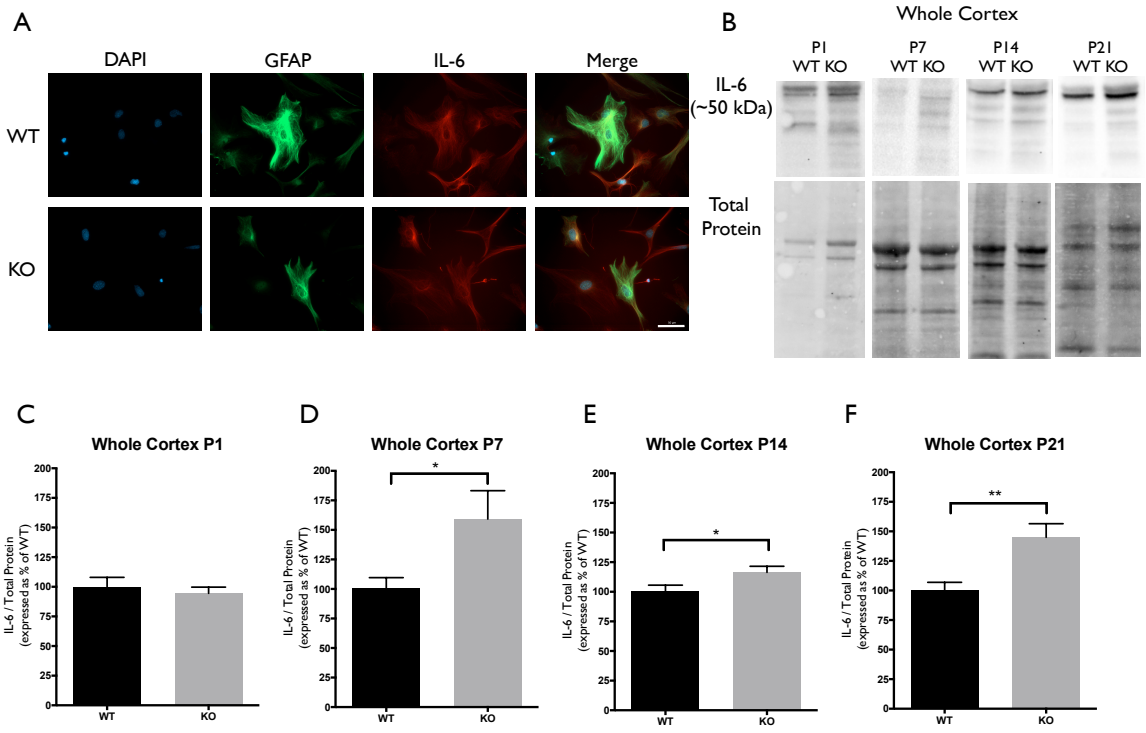
A
DAPI
GFAP
IL-6
Merge
WT
KO
B
Whole Cortex
P1 WT KO
P7 WT KO
P14 WT KO
P21 WT KO
IL-6 (~50 kDa)
Total Protein
C
Whole Cortex P1
D
Whole Cortex P7
E
Whole Cortex P14
F
Whole Cortex P21
IL-6 / Total Protein (expressed as % of WT)
WT
KO

Figure 3: IL-6 expression is significantly increased at postnatal day P7, P14 and P21 in the cortex of *FMR1* KO mice. (A) Cultured cortical astrocytes co-labelled with anti-glial fibrillary acidic protein (GFAP; green), 4', 6-diamidino- 2-Phenylindole (DAPI; blue) and anti-IL-6 (red) after 3 days *in vitro*. Images were obtained using a 40x objective with a Zeiss Axioimager M2. Scale bars=50μm. **(B)** Western blots showing IL-6 expression (~ 50 kDa) in cortical samples containing 30 μg of protein from P1 (6 males and 2 females), P7 (5 males and 3 females), P14 (6 males and 2 females) and P21 (8 males and 0 females) WT and *FMR1* KO mice. Corresponding total protein was used as a loading control. **(C-F)** Cortical expression of IL-6 in WT (black; n=8) and *FMR1* KO (grey; n=8) mice at P1, P7, P14 and P21. Representative bands were normalized to the total protein and expressed as a percentage of the average IL-6 in the WT group. Statistical differences denoted with a single asterisk, $P < 0.05$ and with a double asterisk, $P < 0.01$.

4.2 Cell associated and secreted Tenascin C and IL-6 levels are altered in *FMR1* KO primary astrocyte cultures.

Since TNC is an astrocyte secreted factor, the protein levels in astrocyte conditioned media (ACM) were analyzed and compared between the WT and *FMR1* KO groups. Additionally, cell associated protein levels were also tested to determine if there were any differences between the genotypes. Western blotting experiments revealed an increase of cell associated TNC expression in *FMR1* KO astrocytes (122.8 ± 9.231, $P < 0.05$; n=6/group; Fig. 4A,C). Additionally, an increase of secreted TNC was also noted by *FMR1* KO astrocytes (117.0 ± 4.356, $P < 0.05$; n=6/group; Fig. 4B,C). Each n represented a biological replicate.

As mentioned previously, TNC is a known ligand of TLR4, meaning that activation of TLR4 by TNC may be capable of inducing IL-6 secretion. With differences seen in cell associated and secreted TNC, cell associated and secreted IL-6 protein levels were analyzed. Western blotting experiments revealed changes in cell associated IL-6 expression between the WT and *FMR1* KO astrocytes (167.3 ± 11.61, $P < 0.0001$; n=6/group; Fig. 4D,F). Additionally, secreted IL-6 protein levels were also increased by *FMR1* KO astrocytes (139.8 ± 7.296, $P < 0.001$; n=6/group; Fig. 4E,F). Each n represented a biological replicate.

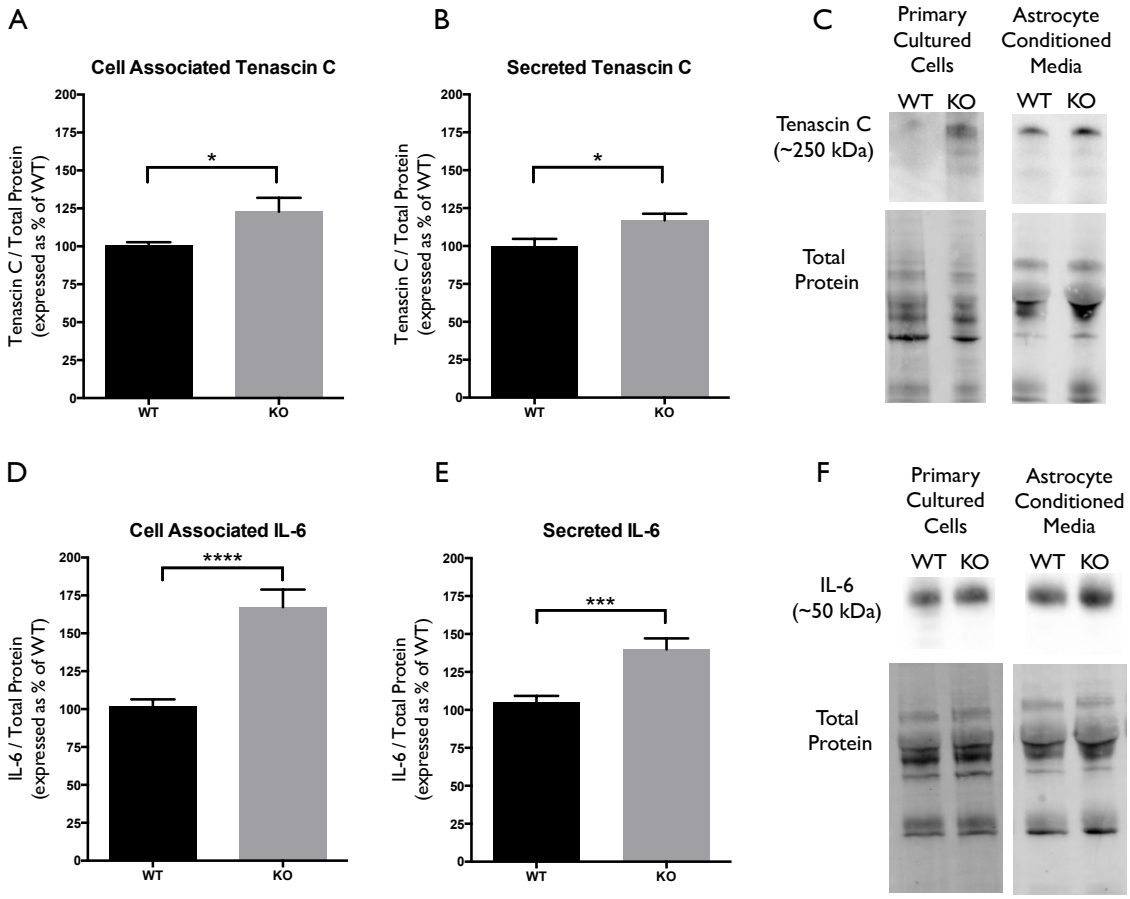
A
Cell Associated Tenascin C
Tenascin C / Total Protein (expressed as % of WT)
200
175
150
125
100
75
50
25
0
*
WT
KO
B
Secreted Tenascin C
Tenascin C / Total Protein (expressed as % of WT)
200
175
150
125
100
75
50
25
0
*
WT
KO
C
Primary Cultured Cells
Astrocyte Conditioned Media
WT KO
WT KO
Tenascin C (~250 kDa)
Total Protein
D
Cell Associated IL-6
IL-6 / Total Protein (expressed as % of WT)
200
175
150
125
100
75
50
25
0
****
WT
KO
E
Secreted IL-6
IL-6 / Total Protein (expressed as % of WT)
200
175
150
125
100
75
50
25
0
***
WT
KO
F
Primary Cultured Cells
Astrocyte Conditioned Media
WT KO
WT KO
IL-6 (~50 kDa)
Total Protein

Figure 4: Cell associated and secreted Tenascin C and IL-6 expression is significantly enhanced *in vitro* by *FMR1* KO astrocyte conditioned media. (A) Cell associated expression of Tenascin C in WT (black; n=6) and *FMR1* KO (grey; n=6) primary astrocyte cultured cells grown for 7 days *in vitro*. Representative bands were normalized to the total protein and expressed as a percentage of the average Tenascin C in the WT group. Statistical differences denoted with a single asterisk, $P < 0.05$. **(B)** Secreted expression of Tenascin C in WT (black; n=6) and *FMR1* KO (grey; n=6) astrocyte conditioned media. Representative bands were normalized to the total protein and expressed as a percentage of the average Tenascin C in the WT group. Statistical differences denoted with a single asterisk, $P < 0.05$. **(C)** Western blots showing Tenascin C expression (~ 250 kDa) in primary astrocyte cultured cells and astrocyte conditioned media. Corresponding total protein was used as a loading control. **(D)** Cell associated expression of IL-6 in WT (black; n=6) and *FMR1* KO (grey; n=6) primary astrocyte cultured cells grown for 7 days *in vitro*. Representative bands were normalized to the total protein and expressed as a percentage of the average IL-6 in the WT group. Statistical differences denoted with four asterisks, $P < 0.0001$. **(E)** Secreted expression of IL-6 in WT (black; n=6) and *FMR1* KO (grey; n=6) astrocyte conditioned media. Representative bands were normalized to the total protein and expressed as a percentage of the average IL-6 in the WT group. Statistical differences denoted with a triple asterisk, $P < 0.001$. **(F)** Western blots showing IL-6 expression (~50 kDa) in primary astrocyte cultured cells and astrocyte conditioned media. Corresponding total protein was used as a loading control.

4.3 Stimulation of TLR4 by exogenous Tenascin C and LPS dysregulated the secretion of IL-6 by WT and *FMR1* KO astrocytes.

Since elevated protein levels of TNC and IL-6 were seen in the ACM from the *FMR1* KO mice, it was essential to determine if this differential expression was due to the activation of TLR4. LPS is a known agonist of TLR4, which is capable of inducing multiple pro-inflammatory molecules; one of those being IL-6. To determine if exogenous TNC was capable of inducing IL-6, we treated WT and *FMR1* KO astrocytes with LPS (10 ug/mL) and exogenous TNC (10 ug/mL) for 3, 6, and 24 h (Fig. 5,6,7). After the indicated time frames, cells and ACM were collected to determine the cell associated and secreted IL-6 levels by a Western blotting.

When WT astrocytes were treated with LPS for 3 h there was an increase of cell associated IL-6 ($P < 0.01$; n=6/group; Fig. 5A), however no effect was seen with exogenous TNC treatment. However, exogenous TNC treatment for 3 h caused an increase in IL-6 protein secretion ($P < 0.05$; n=6/group; Fig. 5B), in both WT and *FMR1* KO astrocytes. Interestingly, only the WT astrocytes increased the level of IL-6 secretion when stimulated by LPS ($P < 0.0001$; n=6/group; Fig. 5B), whereas the *FMR1* KO astrocytes had no change. Additionally, when treated with LPS and exogenous TNC for 6 h, an increase of IL-6 secretion was noted only in the WT astrocytes when compared to the Naive group ($P < 0.001$; n=6/group; Fig. 6B). By 24 h, there were no changes seen in neither cell associated nor secreted IL-6 protein expression (Fig. 7).

4.4 TLR4 antagonist LPS-RS and TLR4 inhibitor TAK242 decreased secretion of IL-6 by *FMR1* KO astrocytes.

LPS-RS is a known antagonist of TLR4, which is capable attenuating pro-inflammatory responses. WT and *FMR1* KO astrocytes were treated with LPS-RS (10 ug/mL) for 3, 6, and 24 h (Fig. 5,6,7,8). After the indicated time frames, cells and ACM were collected to determine cell associated and secreted IL-6 levels by a Western Blot. When *FMR1* KO astrocytes were treated with LPS-RS for 3 h, there was a decrease of cell associated IL-6 ($P < 0.01$; n=6/group; Fig. 5A), when compared to the Naive group. After 3 h treatments with LPS-RS, ACM from WT astrocytes resulted in no difference in IL-6 secretion, however there was less secreted IL-6 from *FMR1* KO astrocytes ($P < 0.0001$, n=6/group; Fig. 5B, 8A) when compared to the Naive group. When astrocytes were treated for 6 h with LPS-RS, a difference in IL-6 secretion was only noted in the *FMR1* KO astrocytes ($P < 0.05$, n=6/group; Fig. 6B, 8A). By 24 h, there was no significant change seen in neither cell associated nor secreted IL-6 protein expression, when the astrocytes were stimulated with LPS-RS (Fig. 7, 8A).

To determine the impact of TLR4 antagonist LPS-RS, as well as inhibitor of TLR4 signalling TAK242 (resatorvid), WT and *FMR1* KO astrocytes were treated with both of the molecules (Fig. 8B). Interestingly, only TAK242 ($P < 0.0001$, n=4; Fig. 8B) and LPS-RS ($P < 0.05$, n=4; Fig. 8B) had the ability to decrease IL-6 secretion in WT astrocytes when compared to Naive WT astrocytes. *FMR1* KO astrocytes were however able to respond to TAK242 and LPS-RS ($P < 0.0001$, n=4; Fig. 8B), as well as TAK242

with the addition of TNC ($P < 0.0001$, n=4; Fig. 8B), when compared to Naive *FMR1* KO astrocytes.

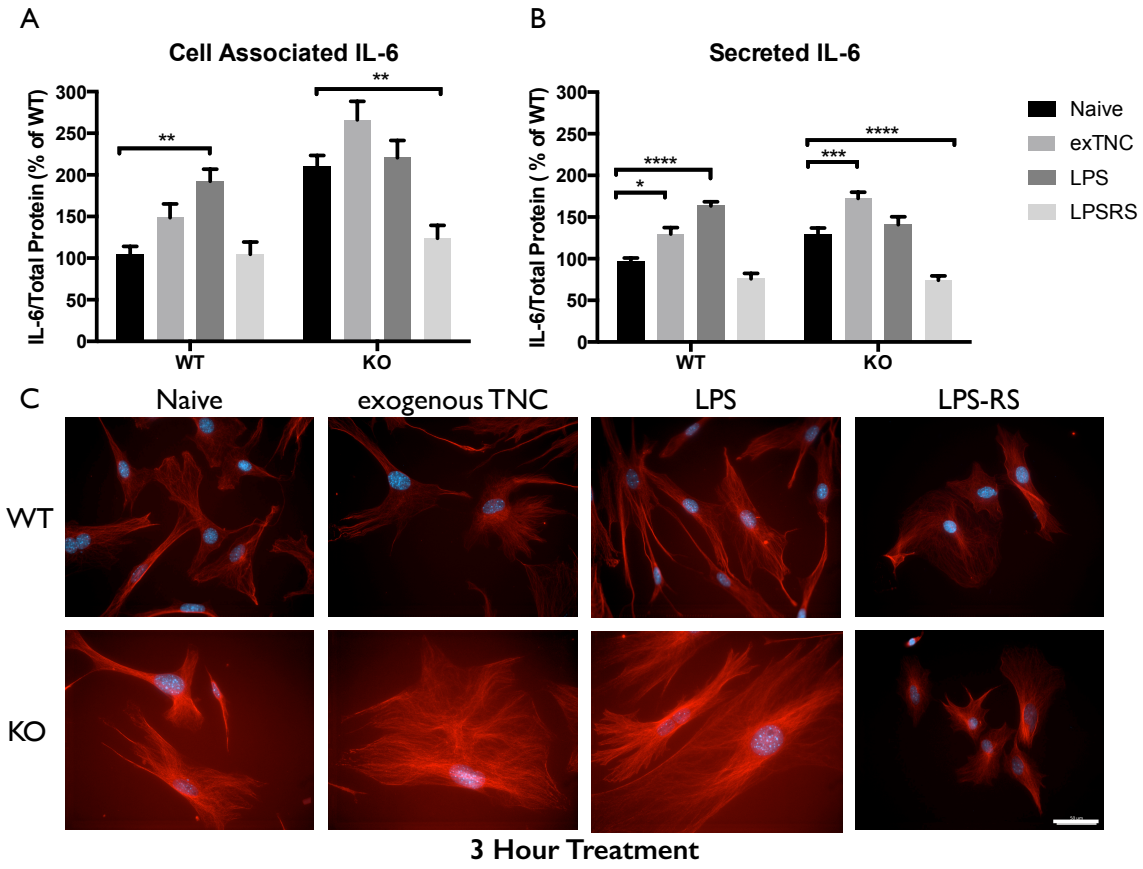
A
Cell Associated IL-6
IL-6/Total Protein (% of WT)
300
250
200
150
100
50
0
**
**
WT
KO
B
Secreted IL-6
IL-6/Total Protein (% of WT)
300
250
200
150
100
50
0
****
*
****
***
WT
KO
Naive
exTNC
LPS
LPSRS
C
Naive
exogenous TNC
LPS
LPS-RS
WT
KO
3 Hour Treatment

Figure 5: Secreted IL-6 expression post a 3-h treatment is significantly altered following TLR4 activation. (A) Cell associated astrocyte expression of IL-6 in WT (n=6/group) and *FMR1* KO (n=6/group) astrocyte cell cultures grown for 7 days *in vitro*. The culture was treated with LPS (10ug/mL), exogenous TNC (10ug/mL), and LPS-RS (10ug/mL) for 3 h prior to collection. Representative bands were normalized to the total protein and expressed as a percentage of the average IL-6 in the WT group. Statistical differences denoted with a with double asterisk, $P < 0.01$. **(B)** Extracellular astrocyte expression of secreted IL-6 in WT (n=6/group) and *FMR1* KO (n=6/group) astrocyte cell cultures grown for 7 days *in vitro*. The culture was treated with LPS (10ug/mL), exogenous TNC (10ug/mL), and LPS-RS (10ug/mL) for 3 h prior to ACM concentration and collection. Representative bands were normalized to the total protein and expressed as a percentage of the average IL-6 in the WT group. Statistical differences denoted with a single asterisk, $P < 0.05$, with a triple asterisk, $P < 0.001$ and with four asterisks, $P < 0.0001$. **(C)** Cultured cortical astrocytes co-labelled with 4', 6-diamidino- 2-Phenylindole (DAPI; blue) and anti-IL-6 (red) after 3 days *in vitro*, following a 3 h treatment. Images were obtained using a 40x objective with a Zeiss Axioimager M2. Scale bars=50μm.

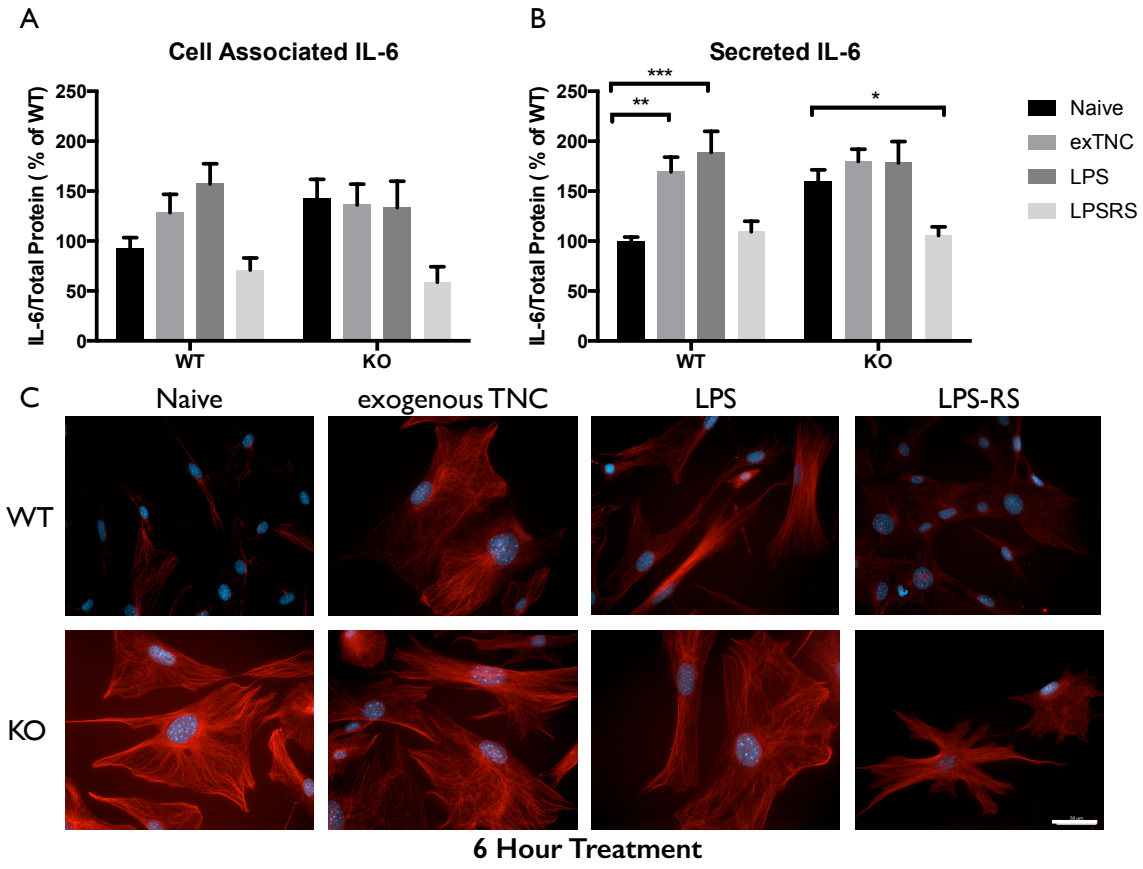
A
Cell Associated IL-6
IL-6/Total Protein (% of WT)
250
200
150
100
50
0
WT
KO
B
Secreted IL-6
***
**
*
Naive
exTNC
LPS
LPSRS
C
Naive
exogenous TNC
LPS
LPS-RS
WT
KO
6 Hour Treatment

Figure 6: Secreted IL-6 expression post a 6-h treatment is significantly altered following TLR4 activation. (A) Cell associated astrocyte expression of IL-6 in WT (n=6/group) and *FMR1* KO (n=6/group) astrocyte cell cultures grown for 7 days *in vitro*. The culture was treated with LPS (10ug/mL), exogenous TNC (10ug/mL), and LPS-RS (10ug/mL) for 6 h prior to collection. Representative bands were normalized to the total protein and expressed as a percentage of the average IL-6 in the WT group. **(B)** Extracellular astrocyte expression of secreted IL-6 in WT (n=6/group) and *FMR1* KO (n=6/group) astrocyte cell cultures grown for 7 days *in vitro*. The culture was treated with LPS (10ug/mL), exogenous TNC (10ug/mL), and LPS-RS (10ug/mL) for 6 h prior to ACM concentration and collection. Representative bands were normalized to the total protein and expressed as a percentage of the average IL-6 in the WT group. Statistical differences denoted with a single asterisk, $P < 0.05$, a double asterisk, $P < 0.01$ and with triple asterisk, $P < 0.001$. **(C)** Cultured cortical astrocytes co-labelled with 4', 6-diamidino- 2-Phenylindole (DAPI; blue) and anti-IL-6 (red) after 3 days *in vitro*, following a 6 h treatment. Images were obtained using a 40x objective with a Zeiss Axioimager M2. Scale bars=50µm.

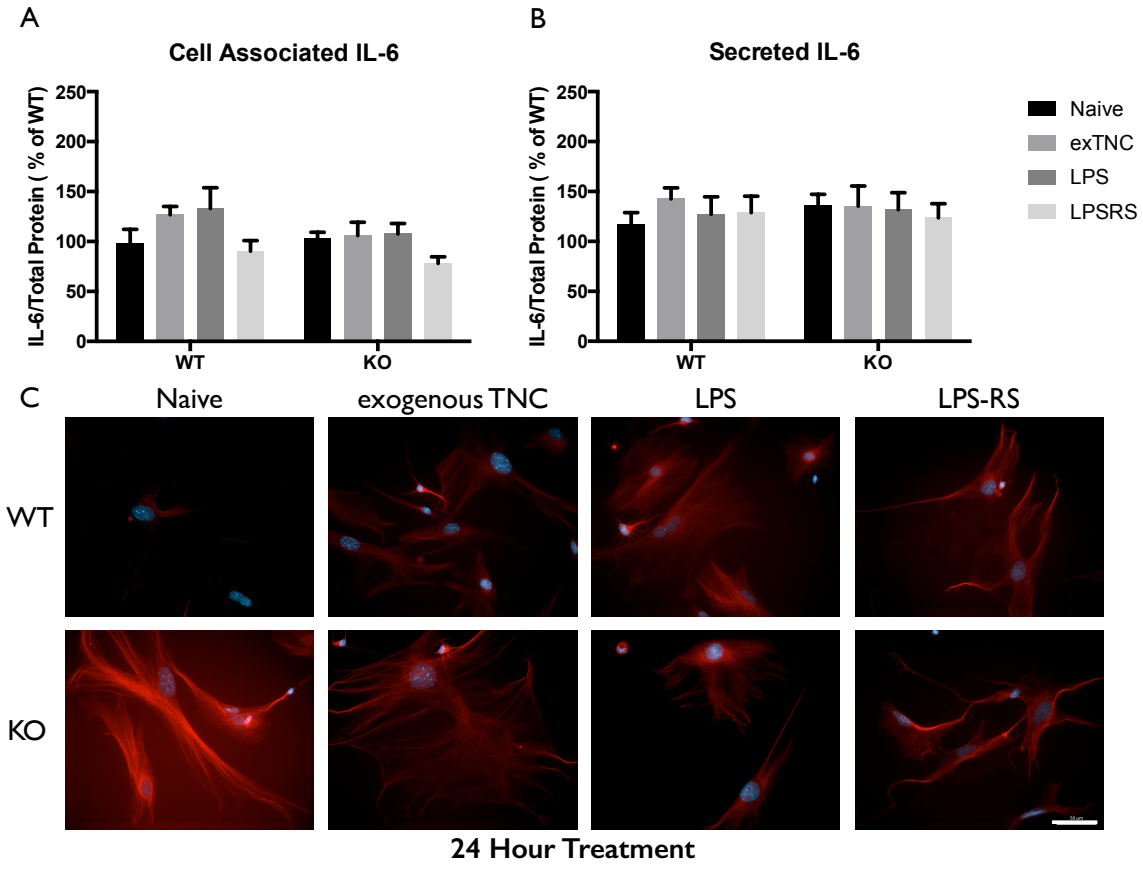
A
Cell Associated IL-6
IL-6/Total Protein (% of WT)
250
200
150
100
50
0
WT
KO
B
Secreted IL-6
IL-6/Total Protein (% of WT)
250
200
150
100
50
0
WT
KO
Naive
exTNC
LPS
LPSRS
C
Naive
exogenous TNC
LPS
LPS-RS
WT
KO
24 Hour Treatment

Figure 7: Secreted IL-6 expression post a 24-h treatment is not significantly altered following TLR4 activation. (A) Cell associated astrocyte expression of IL-6 in WT (n=6/group) and *FMR1* KO (n=6/group) astrocyte cell cultures grown for 7 days *in vitro*. The culture was treated with LPS (10ug/mL), exogenous TNC (10ug/mL), and LPS-RS (10ug/mL) for 24 h prior to collection. Representative bands were normalized to the total protein and expressed as a percentage of the average IL-6 in the WT group. **(B)** Extracellular astrocyte expression of secreted IL-6 in WT (n=6/group) and *FMR1* KO (n=6/group) astrocyte cell cultures grown for 7 days *in vitro*. The culture was treated with LPS (10ug/mL), exogenous TNC (10ug/mL), and LPS-RS (10ug/mL) for 24 h prior to ACM concentration and collection. Representative bands were normalized to the total protein and expressed as a percentage of the average IL-6 in the WT group. **(C)** Cultured cortical astrocytes co-labelled with 4', 6-diamidino- 2-Phenylindole (DAPI; blue) and anti-IL-6 (red) after 3 days *in vitro*, following a 24 h treatment. Images were obtained using a 40x objective with a Zeiss Axioimager M2. Scale bars=50μm.

A

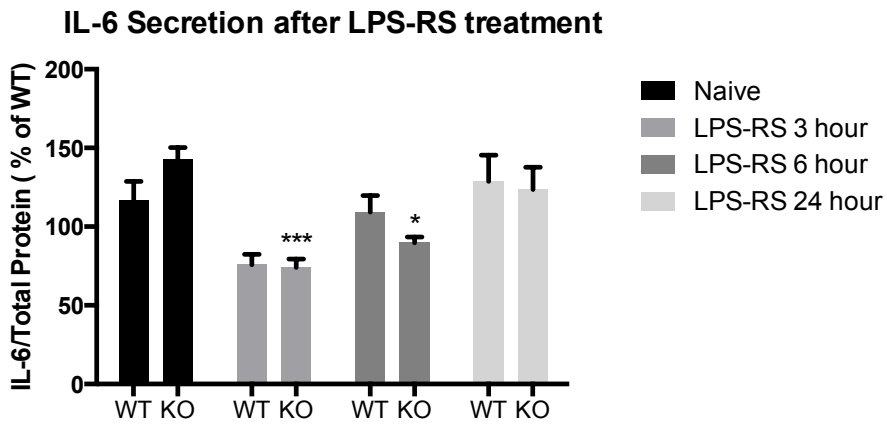
IL-6 Secretion after LPS-RS treatment
IL-6/Total Protein (% of WT)
200
150
100
50
0
***
*
WT KO WT KO WT KO WT KO
Naive
LPS-RS 3 hour
LPS-RS 6 hour
LPS-RS 24 hour

B

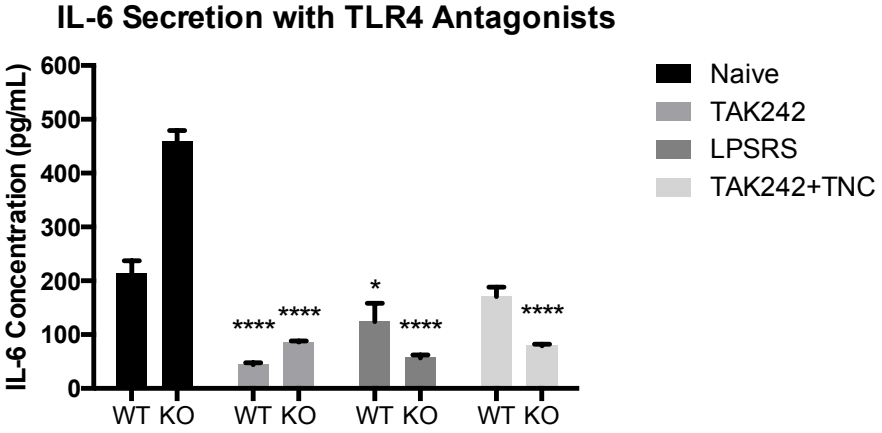
IL-6 Secretion with TLR4 Antagonists
IL-6 Concentration (pg/mL)
600
500
400
300
200
100
0
****
****
*
****
****
WT KO WT KO WT KO WT KO
Naive
TAK242
LPSRS
TAK242+TNC

Figure 8: IL-6 secretion is impacted in both WT and *FMR1* KO astrocytes, when treated with various TLR4 antagonists. (A) Extracellular astrocyte expression of secreted IL-6 in WT (n=6/group) and *FMR1* KO (n=6/group) astrocyte cell cultures grown for 7 days *in vitro*. The culture was treated with LPS-RS (10ug/mL) for 3,6 and 24 h prior to ACM concentration and collection. Statistical differences denoted with a single asterisk, $P < 0.05$. **(B) A)** Analysis of IL-6 in astrocyte conditioned media from WT (n=4/group) and *FMR1* KO (n=4/group) astrocytes grown for 7 days *in vitro*. The culture was treated with TAK242 (5ug/mL), LPS-RS (10ug/mL) and TAK242(5ug/mL) with the addition of TNC (10ug/mL). Statistical differences denoted with a single asterisk, $P < 0.05$ and with four asterisk, $P < 0.0001$.

4.5 *FMR1* KO astrocyte conditioned media increases co-localized excitatory synaptic puncta

Autism spectrum disorders have been speculated to arise from functional changes in neuronal circuitry, and they have been associated with an imbalance in excitatory/inhibitory synaptic transmission. To investigate whether the elevated IL-6 in *FMR1* KO astrocytes, could impact synapse formation we used antibodies against synaptic vesicle proteins. With our previous finding of increased cell associated and secreted IL-6, we used ACM from WT and *FMR1* KO astrocytes to determine the number of excitatory synaptic puncta. Antibodies against VGLUT1 and PSD95 were used to analyze the co-localization of the pre- and post-synaptic markers (Fig. 9). We examined a dramatic increase of co-localized excitatory puncta when WT and *FMR1* KO neurons were supplemented with *FMR1* KO ACM and maintained for 12 days *in vitro* ($P < 0.0001$, n=4, 40 neurons per condition, Fig. 9).

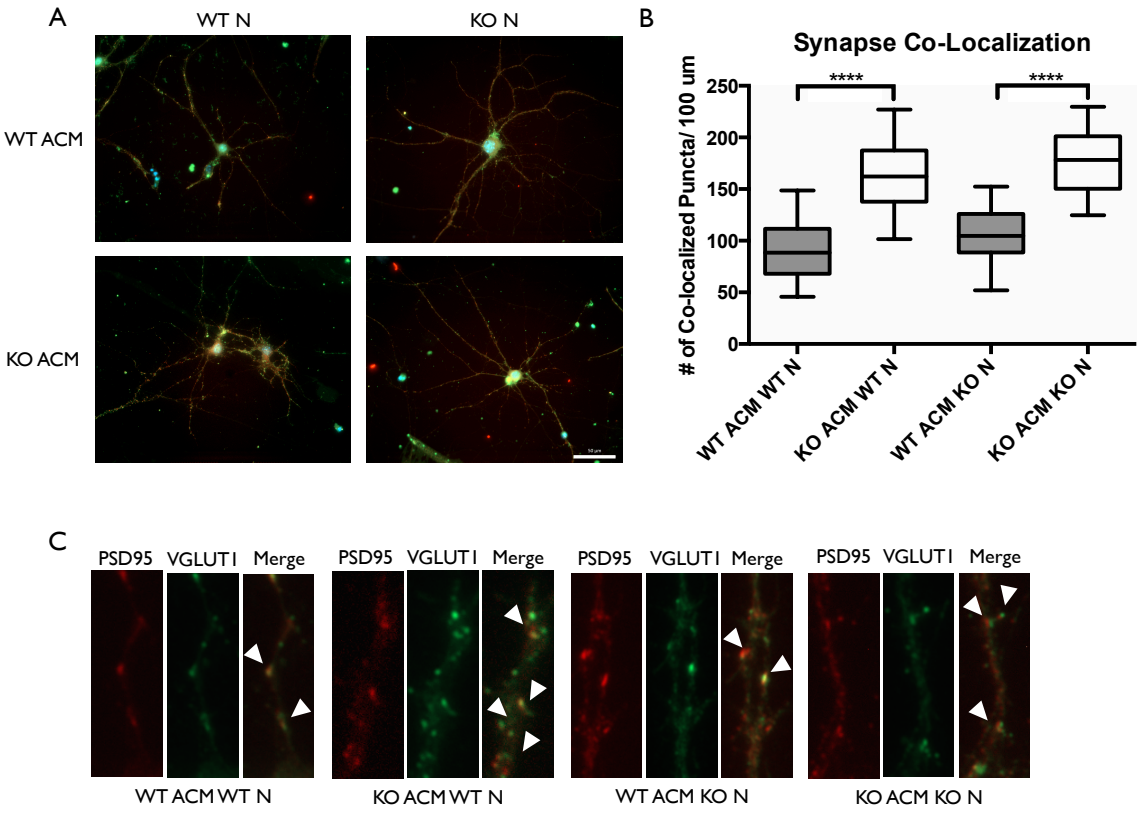
A
WT N
KO N
WT ACM
KO ACM
B
Synapse Co-Localization
# of Co-localized Puncta/100 um
250
200
150
100
50
0
****
****
WT ACM WT N
KO ACM WT N
WT ACM KO N
KO ACM KO N
C
PSD95 VGLUT1 Merge
PSD95 VGLUT1 Merge
PSD95 VGLUT1 Merge
PSD95 VGLUT1 Merge
WT ACM WT N
KO ACM WT N
WT ACM KO N
KO ACM KO N

Figure 9: The number of VGLUT1/PSD95 co-localized puncta of WT and *FMR1* KO neurons was increased when plated with astrocyte conditioned media from *FMR1* KO astrocytes, compared to those plated with media from WT astrocytes. **(A)** WT and *FMR1* KO neurons with astrocyte conditioned media (ACM) from WT and *FMR1* KO astrocytes maintained for 12 days *in vitro*, co-labelled with antibodies against vesicular glutamate transporter-1 (VGLUT1) and post-synaptic density protein 95 (PSD95). **(B)** Measures of intracortical synapse number (identified by the co-localization of VGLUT1 and PSD95 puncta) obtained from cultures containing WT or *FMR1* KO neurons, supplemented with ACM from WT or *FMR1* KO astrocytes (n=4; 40 neurons /condition). Statistical differences denoted with four asterisks, $P<0.0001$. **(C)** WT and *FMR1* KO neurons supplemented with ACM from WT or *FMR1* KO astrocytes and maintained for 12 days *in vitro*. White arrows indicate co-localized PSD95 (red) and VGLUT1 (green) puncta. Images were obtained using a 40x objective with a Zeiss Axioimager M2. Scale bars=50μm.

4.6 Exogenous Tenascin C up-regulates the level of IL-6 receptor in cultured primary astrocytes

The expression of IL-6 receptor was important to analyze in WT and *FMR1* KO astrocytes to determine whether the IL-6 expression changes are also dependent on the receptor expression. Since there were changes of secreted IL-6 when astrocytes were treated with TNC, it was important to determine whether this treatment would also impact IL-6R expression. We examined an increase of IL-6R expression only in *FMR1* KO astrocytes, when treated with exogenous TNC ($P < 0.05$, n=4, Fig. 10).

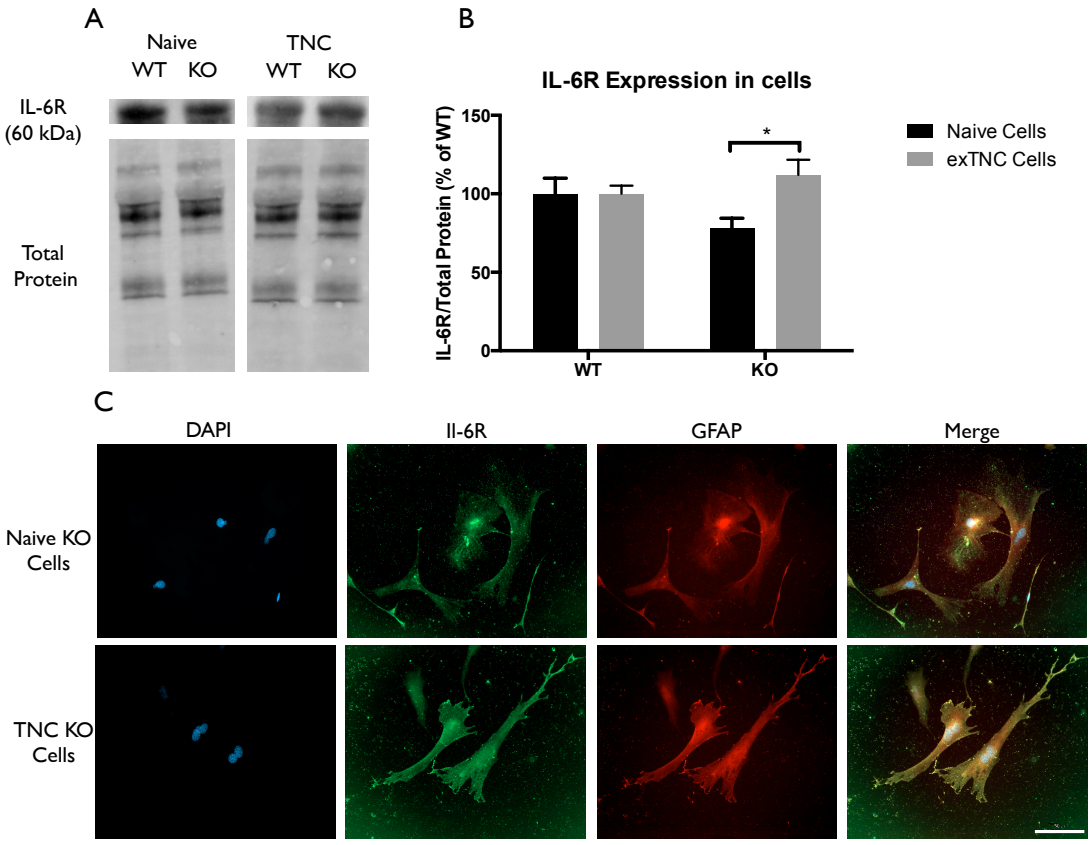
A
Naive
TNC
WT KO WT KO
IL-6R
(60 kDa)
Total
Protein
B
IL-6R Expression in cells
IL-6R/Total Protein (% of WT)
150
100
50
0
*
WT
KO
Naive Cells
exTNC Cells
C
DAPI
Il-6R
GFAP
Merge
Naive KO
Cells
TNC KO
Cells

Figure 10: IL-6R expression is altered in WT astrocytes treated with Tenascin C. (A) Western blots showing IL-6R expression (~ 60 kDa) in samples containing 30 µg of protein from naive and Tenascin C WT and *FMR1* KO primary astrocyte cultures. Corresponding total protein was used as a loading control. **(B)** Cortical expression of IL-6R in WT (black; n=4) and *FMR1* KO (grey; n=4) naive and Tenascin C treated primary astrocyte cultures. Representative bands were normalized to the total protein and expressed as a percentage of the average IL-6 in the WT group. Statistical differences denoted with a single asterisk, $P < 0.05$. **(C)** Cultured cortical astrocytes co-labelled with 4', 6-diamidino- 2-Phenylindole (DAPI; blue), anti-IL-6R (green) and anti-glial fibrillary acidic protein (GFAP; red) after 3 days *in vitro*. Images were obtained using a 40x objective with a Zeiss Axioimager M2. Scale bars=50µm.

4.7 Ratio of phosphorylated STAT3: total STAT3 is elevated after Tenascin C treatment

LPS and other cytokines are known to activate the JAK/STAT pathway, leading to phosphorylation of tyrosine and serine. Therefore, we investigated the response of tyrosine phosphorylation of STAT3 after TNC treatment. To determine the ratio of phosphorylation, Western blotting was done to determine the total STAT3, in additional to phosphorylated STAT3, which was then subsequently divided. The level of STAT3 phosphorylation was tremendously increased when both WT and *FMR1* KO astrocytes were treated with exogenous TNC ($P < 0.001$, n=4, Fig. 11).

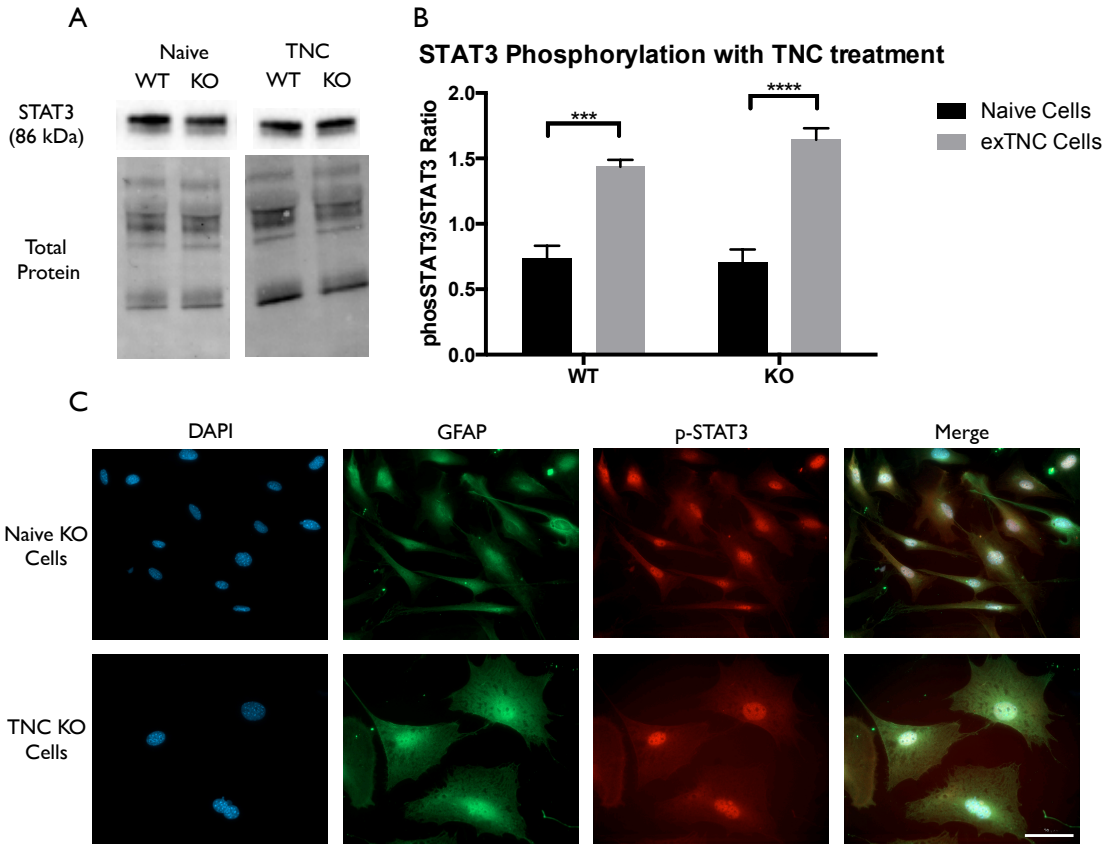
A
Naive
TNC
WT
KO
WT
KO
STAT3
(86 kDa)
Total
Protein
B
STAT3 Phosphorylation with TNC treatment
phosSTAT3/STAT3 Ratio
2.0
1.5
1.0
0.5
0.0
***
****
WT
KO
Naive Cells
exTNC Cells
C
DAPI
GFAP
p-STAT3
Merge
Naive KO
Cells
TNC KO
Cells

Figure 11: Phosphorylation of STAT3 is altered in WT and *FMR1* KO astrocytes when treated with Tenascin C. (A) Western blots showing phosphorylated STAT3 (p-STAT3) expression (~ 86 kDa) in samples containing 30 µg of protein from naive and Tenascin C WT and *FMR1* KO primary astrocyte cultures. Corresponding total protein was used as a loading control. **(B)** Expression of p-STAT3 in WT (black; n=4) and *FMR1* KO (grey; n=4) naive and Tenascin C treated primary astrocyte cultures. Representative bands were normalized to the total protein and expressed as a percentage of the average p-STAT3 in the WT group. Statistical differences denoted with a triple asterisk, $P < 0.001$ and four asterisks, $P < 0.0001$. **(C)** Cultured cortical astrocytes co-labelled with 4', 6-diamidino- 2-Phenylindole (DAPI; blue), anti-glial fibrillary acidic protein (GFAP; green) and anti-p-STAT3 (red) after 3 days *in vitro*. Images were obtained using a 40x objective with a Zeiss Axioimager M2. Scale bars=50µm.

4.8 STAT3 knockdown in WT and *FMR1* KO astrocytes

To examine the mechanisms regulating IL-6, we tested whether STAT3 was capable of impacting IL-6 secretion in WT and *FMR1* KO astrocytes. IL-6 production in glia induced with LPS treatment, has been previously reduced by downregulation of STAT3 expression by siRNA and by pharmacological inhibition of STAT3. We wanted to determine whether STAT3 participates in IL-6 production, as seen by the secretion of IL-6, determine by an ELISA. We determined that downregulation of STAT3 had the ability to decrease IL-6 secretion in both WT ($P < 0.05$, n=4, Fig. 12A,B,C) and *FMR1* KO astrocytes ($P < 0.001$, n=4, Fig. 12A,B,C). Additionally, both WT and *FMR1* KO astrocytes transfected with STAT3 siRNA and treated with exogenous TNC for 3 hours prior to collection exhibited lower levels of IL-6 secretion ($P < 0.05$, n=4, Fig. 12C). Neither siRNA transfection nor treatment had impact on cell viability (Fig. 12D). Additionally, transfection efficacy was determined to be approximately 40-45% in both WT and *FMR1* KO astrocytes.

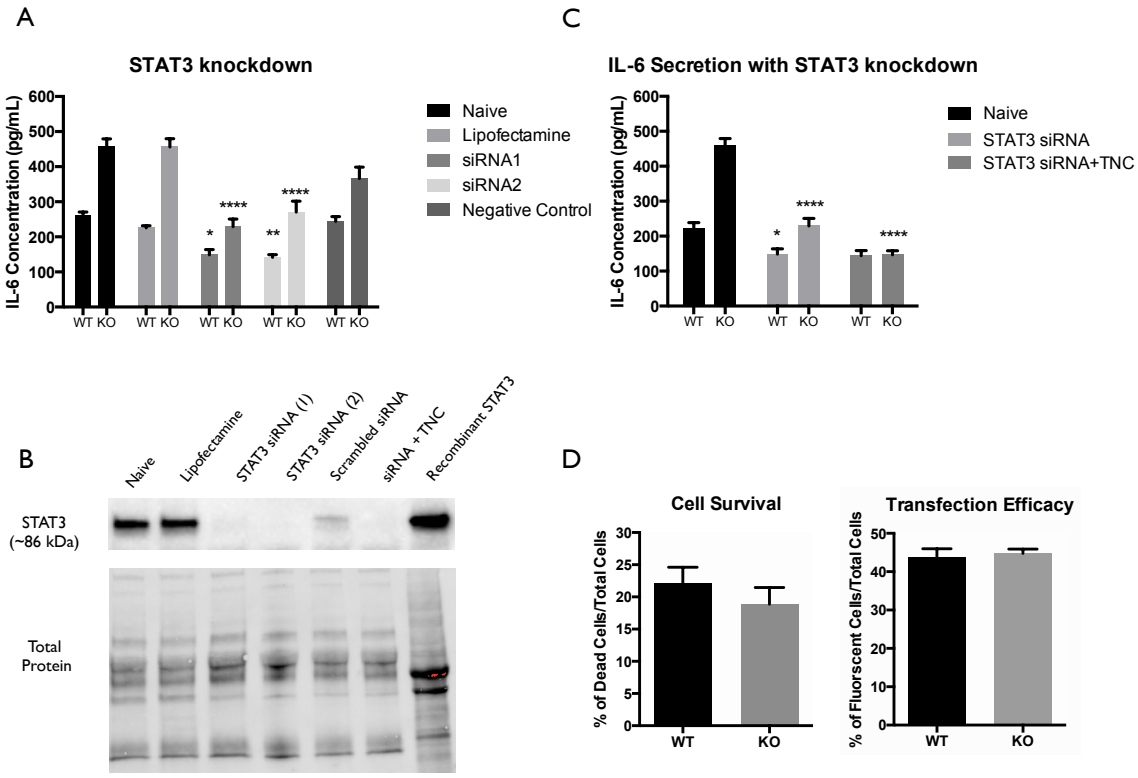
A
STAT3 knockdown
IL-6 Concentration (pg/mL)
600
500
400
300
200
100
0
WT KO WT KO WT KO WT KO WT KO
*
**
****
****
Naive
Lipofectamine
siRNA1
siRNA2
Negative Control
C
IL-6 Secretion with STAT3 knockdown
IL-6 Concentration (pg/mL)
WT KO WT KO WT KO
*
****
****
Naive
STAT3 siRNA
STAT3 siRNA+TNC
B
Naive
Lipofectamine
STAT3 siRNA (1)
STAT3 siRNA (2)
Scrambled siRNA
siRNA + TNC
Recombinant STAT3
STAT3
(~86 kDa)
Total
Protein
D
Cell Survival
% of Dead Cells/Total Cells
30
25
20
15
10
5
0
WT
KO
Transfection Efficacy
% of Fluorscent Cells/Total Cells
50
40
30
20
10
0
WT
KO

Figure 12: IL-6 secretion is significantly decreased by astrocytes after STAT3 siRNA knock-down. (A) Analysis of IL-6 in astrocyte conditioned media from WT and FMR1 KO astrocytes transfected with Lipofectamine alone, with two different STAT3 siRNA, and a scrambled siRNA. **(B)** Western blots showing phosphorylated STAT3expression (~ 86 kDa) in samples containing 30 µg of protein from *FMR1* KO primary astrocyte cultures. Corresponding total protein was used as a loading control. **(C)** Analysis of IL-6 in astrocyte conditioned media from WT and FMR1 KO astrocytes transfected with Lipofectamine and STAT3 siRNA, and treated with exogenous TNC. **(D)** Analysis of cell survival and tranfection efficacy after transfection in both WT and *FMR1* KO astrocytes determined by the number of fluorescently labeled cells.

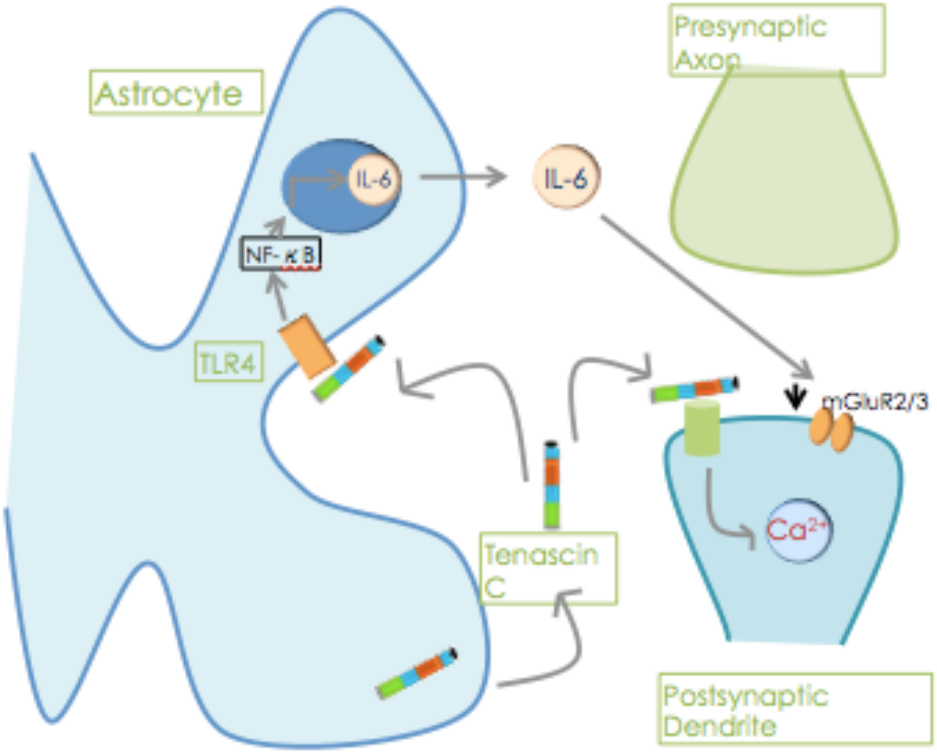
Astrocyte
Presynaptic Axon
IL-6
IL-6
NF-κB
TLR4
mGluR2/3
Ca2+
Tenascin C
Postsynaptic Dendrite

Figure 13: Proposed mechanism of the TNC-TLR4-IL-6 axis. Mechanism of TNC binding to TLR4 and inducing the cell associated and secreted IL-6. Up-regulated IL-6 has been implicated in synaptic regulation, as noted by a decrease of mGluR2/3, which has also been investigated in the valproate induced rat model of autism.

CHAPTER FIVE

DISCUSSION AND CONCLUSION

The first few weeks of postnatal development consist of highly regulated events involving synapse growth, formation and pruning (Faissner et al. 2010; Gatto and Broadie 2010). This complex and dynamic process requires a coordinated exchange of signals from neurons and glia (Cheng, Sourial, and Doering 2012). In many disorders of the nervous system, the structure and function of synapse formation is strained, and thereby translated to cognitive and behavioural deficits (Cheng, Sourial, and Doering 2012; Contractor, Klyachko, and Portera-Cailliau 2015). Recently, astrocytes have emerged as an essential cell type for the regulation of synaptic connectivity. Given their close proximity to neurons, astrocytes are able to regulate synapse formation through secreted and contact mediated factors (Faissner et al. 2010; Jones and Bouvier 2014). A multitude of soluble factors secreted by astrocytes are responsible for synaptogenesis and synaptic function. Previous research from our lab has demonstrated that Hevin, SPARC and Thrombospondin-1 (TSP-1) are soluble factors that can rescue afferent spine morphology in the *FMR1* KO mouse model (Wallingford et al. 2017; Cheng, Lau, and Doering 2016; Shelley Jacobs and Doering 2010). In particular, TSP-1 was found to be decreased in *FMR1* KO hippocampal astrocyte cultures (Cheng, Lau, and Doering 2016). Correspondingly, *FMR1* KO neuron cultures exhibited morphological deficits in synaptic formation (Cheng, Lau, and Doering 2016). Additionally, hevin was found to be up regulated in cortical tissue and in primary astrocytes cultures in the *FMR1* KO model, meanwhile SPARC expression was found to be decreased (Wallingford et al. 2017). Thus, the discovery of other astrocyte secreted factors is essential to understand the extracellular impact of the environment on neurons.

5.1 TNC, TLR4 and IL-6 expression in the cortex and primary astrocyte cultures in WT and *FMR1* KO astrocytes

In this study, we examined the interaction and activation of TLR4 by the astrocyte secreted factor, TNC. Such activation would result in the synthesis of pro-inflammatory cytokines such as IL-6, which is ultimately known to be involved in the formation of excitatory synapses (Hongen Wei et al. 2011; Tancredi et al. 2000). This study is the first to determine the relationship between TNC and IL-6, through the activation of TLR4 in astrocytes and in FXS. Interestingly, we discovered an up-regulation of TNC and IL-6 in the *FMR1* KO cortices at P14 and P21 (Fig. 1E,F and Fig. 3 E,F). TNC expression was found to be down-regulated at P7 (Fig. 1D), potentially due to upstream factors such as intracellular signals that are controlled by soluble factors, integrins and other mechanical forces (Lloyd and Jones 2000). Another mechanism for the elevated TNC expression could be due to astrocyte reactivity. First evidence of astrocyte reactivity in the FXS mouse model has been shown by the Pacey lab, making this a viable explanation as to why there is an increase of TNC in the *FMR1* KO model (Pacey et al. 2015). Additionally, developmental expression of TNC was found to be down-regulated in WT astrocytes, however this does not seem to be the case for TNC expression by *FMR1* KO astrocytes. Thus, these results do complement previous findings that TNC is developmentally down-regulated in a normal functioning system (Joester and Faissner 1999). Interestingly, IL-6 expression still remained elevated at P7, even though TNC expression was found to be down-regulated (Fig. 1 and Fig. 3). This could be explained by IL-6 regulation through the JAK/STAT3 pathway, as IL-6 has the potential to recruit

JAK and phosphorylate STAT3, thus increasing the production and secretion of IL-6 (Greenhill et al. 2011; Beurel et al. 2009; Samavati et al. 2009). However, since we bred WT and *FMR1* KO mice from separate colonies, we cannot exclude the possibility that the effects we observe are influenced by differences in maternal care.

In rodents, the critical time-span for synaptogenesis occurs in the first two weeks of life, while maturation of the synapses occurs approximately between P14 and P21 (Cheng, Sourial, and Doering 2012; Gatto and Broadie 2010). The elevation of TNC protein levels at these critical time points may suggest that there is more involvement of TNC in synaptogenesis than previously investigated. The maintenance of plasticity in the brain correlates with the expression of extracellular glycoproteins such as TNC, with recent studies suggesting that TNC may be involved in synapse function through the modulation of intracellular Ca^{2+} levels (Faissner et al. 2010; Dityatev and Schachner 2003; Barros, Franco, and Mu 2017).

TNC is expressed at low amounts in healthy tissue, although up-regulation is seen in tissue injury and during states of inflammation (I. A. Udalova et al. 2011; Stamenkovic et al. 2016). This has been shown to trigger TLR4 activation in macrophages, dendritic cells, neutrophils and synovial fibroblasts (Midwood et al. 2009; Hongen Wei et al. 2011). In the CNS, there is a vast amount of TLR4 expression by neurons, microglia, as well as astrocytes (Shen et al. 2016; Gorina et al. 2011). This study determined that the expression levels of cortical TLR4 are similar in both the WT and *FMR1* KO mouse

model (Fig. 2). A recent study suggested that astrocytic activation of TLR4 through the Myd88 mediated pathway by LPS, induces pro-inflammatory cytokines and promotes excitatory synaptogenesis in the second postnatal week in mice (Shen et al. 2016). This ultimately prompted the question whether TNC is capable of activating TLR4 in astrocytes to promote excitatory synaptogenesis through cytokine synthesis.

The pro-inflammatory cytokine of interest in this study was IL-6, as it has been implicated in ASD and in the formation of excitatory synapses (Hongen Wei et al. 2011, 2012). Although primary functions of IL-6 have been linked to neuroimmune responses that seem to be involved in physiological brain development, a recent study has suggested that IL-6 is increased in the cerebellum of autistic patients, which in turn alters synapse formation (Hongen Wei et al. 2011). Additionally, primary hippocampal neuron cultures, treated with exogenous IL-6 have shown to significantly reduce Group II-metabotropic receptors (mGluR2/3) and L-type Ca^{2+} channels (Vereyken et al. 2007). This is of interest since in the valproate-induced model of autism, mGluR2/3 protein and mGluR2 mRNA has been shown to be reduced (Shelley Jacobs and Doering 2010). Major changes in Ca^{2+} signalling have also been noted due to the absence of FMRP, which may result from the reduced mRNA for the L-type Ca^{2+} channels (Contractor, Klyachko, and Portera-Cailliau 2015).

5.2 WT and *FMR1* KO astrocyte response to immunological challenges

The TLR receptor family has been mediating host defense infection and injury by recognizing pathogen and damage associated molecular patterns (PAMPS and DAMPS)

(Trotta et al. 2014). Upon activation with bacterial endotoxin LPS, TLRs promote responses such as induction of cytokines mediated by protein tyrosine kinases, mitogen-activated protein kinases (MAPKs) and transcription factors such as nuclear factor κB (NFκB) (Gorina et al. 2011). To determine if *FMR1* KO astrocytes respond differently to an immunological challenge, we treated WT and *FMR1* KO astrocytes with LPS and examined the cultures with Western blots 3, 6, and 24 h post-treatment (Fig. 5-7). Only the WT astrocytes responded to LPS stimulation after 3 and 6 h treatments, as seen by an increase of secreted IL-6 in contrast to the *FMR1* KO astrocytes, where secreted levels remained comparable to the Naive group. This complements a previous report which observed no alterations in cultured primary microglia lacking FMRP when treated for 6 h with LPS (100 ng/mL) (Yuskaitis, Beurel, and Jope 2011). To further analyze how TLR4 is capable of IL-6 induction through endogenous stimuli such as TNC, we treated WT and *FMR1* KO astrocytes with TNC for 3, 6, and 24 h, and analyzed IL-6 protein expression with Western blotting (Fig. 5-7). We have shown here that TNC is capable of activating TLR4 in the astrocyte and promoting cytokine secretion in WT astrocytes. In particular, the FBG domain has been identified as the domain to cause spontaneous release of IL-6 via the MyD88 dependent pathway (Midwood et al. 2009). *FMR1* KO astrocytes seemed to respond to exogenous TNC treatment only when treated for 3 h (Fig. 5B). Since the *FMR1* KO astrocytes already have increased cell associated and secreted TNC levels, the system may have become oversaturated thus being unable to respond to the agonist when treated for longer periods of time (Fig. 6B and Fig 7B). To determine whether *FMR*1 KO astrocytes respond differently to TLR4 antagonist treatments, both WT and *FMR1* KO

astrocytes were treated with LPS-RS for 3,6, and 24 h. Interestingly, only *FMR1* KO astrocytes had the ability to decrease the amount of secreted IL-6 when the TLR4 receptor was antagonized for 3 and 6 h (Fig. 5B, 6B, 8A). Antagonist treatment effects were not seen in WT astrocytes potentially because *FMR1* KO astrocytes were more sensitive to the LPS-RS treatment. By 24 h, both the WT and *FMR1* KO may have become desensitized as no treatment effect is seen for either the TLR4 agonist and antagonist treatments (Fig. 7, 8A).

To further explore the impact that TLR4 antagonists have on IL-6 secretion, we treated the WT and *FMR1* KO astrocytes with an additional pharmacological antagonist TAK242. This pharmacological compound is an inhibitor of TLR4 signalling, that functions by binding to the intracellular domains of TLR4 (Matsunaga et al. 2011). To evaluate whether TAK242 suppresses cytokine levels, a double blind, placebo-controlled study was conducted for the treatment of severe sepsis, and was determined to decrease IL-6 plasma levels relative to baseline (Matsunaga et al. 2011). Taking this into consideration, it was important to determine whether TAK242 in an *in vitro* model could impact IL-6 secretion. TAK242 treatment in both WT and *FMR1* KO astrocytes was able to dramatically decrease IL-6 secretion (Fig. 8B). Additionally, TAK242 treatment was able to withstand the addition of TNC in *FMR1* KO astrocytes, and still maintain low IL-6 levels (Fig. 8B). This suggests that TAK242 may be a promising drug candidate, capable of reducing secreted IL-6, which could decrease excitatory synapse formation.

5.3 Increase of VGlut1/PSD95 synapse co-localization of WT and *FMR1* KO neurons supplemented with conditioned media from *FMR1* KO astrocytes

Synapses are intracellular junctions, which mediate neuronal connections. They rely on proper formation, maintenance and function, that are dependent by the number, type and connectivity patterns of neuronal circuitries (Chung, Allen, and Eroglu 2015). Improper synapse number, which ultimately leads to functional dysregulation, may cause neurodevelopmental disorders such as FXS. Keeping in mind the potential role that IL-6 may play in synaptic development (Hongen Wei et al. 2011), we sought to determine whether WT and *FMR1* KO neurons developed a different number of synaptic connections when cultured with astrocyte conditioned media from *FMR1* KO astrocytes, compared to those cultured with astrocyte conditioned media from WT astrocytes. We co-labeled these neurons with antibodies against VGLUT1 and PSD95. Intracortical synaptic connections were determined by co-localization of the pre- and post- synaptic markers. Interestingly we found an increased number of excitatory synaptic connections when WT and *FMR1* KO neurons were supplemented with astrocyte conditioned media from *FMR1* KO astrocytes (Fig. 9). It is worth noting that astrocyte conditioned media from WT astrocytes did not impact synaptic formation (Fig.9).

It is well established that abnormal spine morphology and density are the major players in FXS research, however, only a handful of studies directly quantify the changes in excitatory synapses (Yang et al. 2016; Pfeiffer and Huber 2009; Contractor, Klyachko, and Portera-Cailliau 2015). To study the changes of excitatory synaptic density in more

detail, we focused on the co-localization of VGLUT1 and PSD95. VGLUT1 is expressed in the majority of cortical-cortical synapses, in particular, these excitatory synaptic connections have been found to be elevated in layer IV and layer V of the mouse somatosensory cortex in FXS (G. X. Wang, Smith, and Mourrain 2014). Since FXS is associated with hypersensitivity to sensory stimuli (Gatto and Broadie 2010), an altered cortical-cortical connectivity could explain the deficits of processing sensory information.

The complexity of neuronal connections is dependent on the modulation of cell adhesion molecules (CAMs), which regulate synapse formation, maturation and plasticity (McGeachie, Cingolani, and Goda 2011; Lee, Shim, and Kaang 2013). Recently, IL-6 over-expression in granule cells was found to affect cell adhesion and migration, which suggests that IL-6 could be implicated in the function of CAMs (Hongen Wei et al. 2011). In our study we have found that cell associated and secreted IL-6 is elevated in *FMR1* KO astrocytes, which further supports the hypothesis that IL-6 has an impact on CAMs. Additionally, TNC is also known to interact directly with CAMs (Zacharias, Norenberng, and Rathjen 1999; Rigato et al. 2002), supporting the argument that both TNC and IL-6 are implicated in synaptic development.

Here, we not only show that elevated levels of endogenous TNC is present in the *FMR1* KO astrocytes, but also that exogenous TNC is capable of inducing secretion of IL-6. With already elevated secreted levels of IL-6 present in astrocytes lacking FMRP, it was crucial to determine if this was the doing of TNC. Understanding the mechanism by

which endogenous activators of TLR4 such as TNC mediate the secretion of IL-6 and other cytokines may help determine which astrocyte secreted factors and to what extent these factors impact synaptic dysregulation. Our findings thus show that an imbalance of astrocyte secreted factors could result in an imbalance of neuronal circuitries in FXS. Further experiments involving the NF-κB pathway, the JAK/STAT3 signaling pathway and integrin contribution could further provide evidence to support the hypothesis of IL-6 being one of these important astrocyte secreted factors that partake in synapse development.

5.4 IL-6 secretion is dependent on STAT3 activation

To determine whether the increase of IL-6 secretion was solely dependent on the TNC-TLR4-IL-6 axis, it was important to investigate the effect of STAT3 activation. As seen in Figure 11, it was determined that STAT3 phosphorylation is impacted by the addition of exogenous TNC. Tyrosine phosphorylation of STAT3 is an event that occurs in response to LPS, thus it was interesting to note that tyrosine phosphorylation is also impacted by TNC. Ultimately, the NF-kB pathway plays the central role for IL-6 and other cytokine production (A. Udalova et al. 2016; Erta, Quintana, and Hidalgo 2012), however STAT3 has been implicated in inflammatory signalling cascades triggered by LPS (Samavati et al. 2009), and potentially also by TNC.

Since STAT3 activation requires active GSK3 (Beurel et al. 2009), which is know to be up-regulated in the FXS brain (Yuskaitis, Beurel, and Jope 2011), it was important

to test whether IL-6 secretion was reduced by STAT3 siRNA. Our findings indicate that the inhibition of STAT3 provide mechanisms to reduce IL-6 secretion by both WT and *FMR1* KO astrocytes (Fig. 12). Most importantly, IL-6 secretion remained decreased with the siRNA STAT3 knockdown and addition of exogenous TNC (Fig. 12C). These results indicate that TNC alone is not sufficient to increase IL-6 secretion in astrocytes, and that a multitude of pathways intervene. GSK3 is also known to be required for IL-6 production, thus future studies investigating the impact of a GSK3 knockdown on IL-6 secretion in *FMR1* KO astrocytes is required to fully understand this mechanism. These findings likely signify the action of STAT3 in promoting IL-6 production, which may ultimately lead to the imbalance of IL-6 in *FMR1* KO astrocytes, making it one of the important pathways that partake in synapse development.

5.5 Conclusion

In conclusion, our study demonstrates that TNC and IL-6 are both significantly increased in the *FMR1* KO cortex and *FMR1* KO astrocytes at various stages of cortical development. We also showed that TNC has the capability of inducing the secretion of IL-6 in WT and *FMR1* KO astrocytes *in vitro*, by which the relationship exists through TLR4. This study also investigated how *FMR1* KO astrocytes react to TLR4 agonists and antagonist in comparison to WT astrocytes. We speculate that the *FMR1* KO system is oversaturated by TNC, thus being unable to affect IL-6 secretion when treated with additional TLR4 agonists for long periods of time. We also speculate that *FMR1* KO astrocytes are more sensitive to some treatments such as LPS-RS. Ultimately, we can

confirm the importance of astrocyte secreted factors in synaptic formation and development, however additional experiments are required to determine to what extent this process is driven by IL-6. These findings suggest that elevated IL-6, which has been previously noted in the autistic brain, could be the contributing factor in abnormal synapse formation, as shown by an increase of excitatory synapses in FXS, which would ultimately contribute to the development of FXS.

REFERENCES

Arsenault, Jason, Shervin Gholizadeh, Yosuke Niibori, Laura K Pacey, Sebok K Halder, Enea Koxhioni, Ayumu Konno, Hirokazu Hirai, and David R Hampson. 2016. "FMRP Expression Levels in Mouse Central Nervous System Neurons Determine Behavioral Phenotype." *Human Gene Therapy* 27 (12): 982–96. doi:10.1089/hum.2016.090.

Barros, Claudia S, Santos J Franco, and Ulrich Mu. 2017. "Extracellular Matrix : Functions in the Nervous System," 1–25.

Beurel, Eléonore, Richard S Jope, RS Hotchkiss, IE Karl, J Cohen, R Green, LK Scott, et al. 2009. "Lipopolysaccharide-Induced Interleukin-6 Production Is Controlled by Glycogen Synthase Kinase-3 and STAT3 in the Brain." *Journal of Neuroinflammation 2009 6:1* 6 (1): 138–50. doi:10.1186/1742-2094-6-9.

Cheng, Connie, Sally K M Lau, and Laurie C Doering. 2016. "Astrocyte-Secreted Thrombospondin-1 Modulates Synapse and Spine Defects in the Fragile X Mouse Model." *Molecular Brain* 9 (1). Molecular Brain: 74. doi:10.1186/s13041-016-0256-9.

Cheng, Connie, Mary Sourial, and Laurie C. Doering. 2012. "Astrocytes and Developmental Plasticity in Fragile X." *Neural Plasticity* 2012. doi:10.1155/2012/197491.

Chung, Won-Suk, Nicola J Allen, and Cagla Eroglu. 2015. "Astrocytes Control Synapse Formation, Function and Elimination." *Cold Spring Harbor Perspectives in Biology* 7: 1–18. doi:10.1101/cshperspect.a020370.

Contractor, Anis, Vitaly A. Klyachko, and Carlos Portera-Cailliau. 2015. "Altered Neuronal and Circuit Excitability in Fragile X Syndrome." *Neuron* 87 (4). Elsevier Inc.: 699–715. doi:10.1016/j.neuron.2015.06.017.

Dityatev, Alexander, and Melitta Schachner. 2003. "Extracellular Matrix Molecules and Synaptic Plasticity." *Nat Rev Neurosci* 4 (6): 456–68. doi:10.1038/nrn1115.

Duy, Phan Q, and Dejan B. Budimirovic. 2017. "FRAGILE X SYNDROME : LESSONS LEARNED FROM THE MOST TRANSLATED." *Translational Neuroscience*, 7–8. doi:10.1515/tnsci-2017-0002.

Erta, María, Albert Quintana, and Juan Hidalgo. 2012. "Interleukin-6, a Major Cytokine in the Central Nervous System." *International Journal of Biological Sciences* 8 (9): 1254–66. doi:10.7150/ijbs.4679.

Faissner, Andreas, Martin Pyka, Maren Geissler, Thomas Sobik, Renato Frischknecht, Eckart D. Gundelfinger, and Constanze Seidenbecher. 2010. "Contributions of Astrocytes to Synapse Formation and Maturation - Potential Functions of the Perisynaptic Extracellular Matrix." *Brain Research Reviews* 63 (1–2). Elsevier B.V.: 26–38. doi:10.1016/j.brainresrev.2010.01.001.

Garcia Bueno, B., J. R. Caso, J. L M Madrigal, and J. C. Leza. 2016. "Innate Immune Receptor Toll-like Receptor 4 Signalling in Neuropsychiatric Diseases." *Neuroscience and Biobehavioral Reviews* 64. Elsevier Ltd: 134–47. doi:10.1016/j.neubiorev.2016.02.013.

Gatto, Cheryl L., and Kendal Broadie. 2010. "Genetic Controls Balancing Excitatory and Inhibitory Synaptogenesis in Neurodevelopmental Disorder Models." *Frontiers in*

Synaptic Neuroscience 2 (JUN): 1–19. doi:10.3389/fnsyn.2010.00004.

Giblin, Sean P., and Kim S. Midwood. 2015. "Tenascin-C: Form versus Function." *Cell Adhesion and Migration* 9 (1–2): 48–82. doi:10.4161/19336918.2014.987587.

Gorina, Roser, Miriam Font-Nieves, Leonardo Márquez-Kisinousky, Tomàs Santalucia, and Anna M. Planas. 2011. "Astrocyte TLR4 Activation Induces a Proinflammatory Environment through the Interplay between MyD88-Dependent NFκB Signaling, MAPK, and Jak1/Stat1 Pathways." *Glia* 59 (2): 242–55. doi:10.1002/glia.21094.

Greenhill, C J, S Rose-John, R Lissilaa, W Ferlin, M Ernst, P J Hertzog, A Mansell, and B J Jenkins. 2011. "IL-6 Trans-Signaling Modulates TLR4-Dependent Inflammatory Responses via STAT3." *J Immunol* 186 (2): 1199–1208. doi:10.4049/jimmunol.1002971.

Hatton, Deborah D, Edward Bucldey, Ave Lachiewicz, and Jane Roberts. 1998. "Ocular Status of Boys With Fragile X Syndrome : A Prospective Study," no. October: 298–302.

Henneberger, Christian, and Christian Steinhäuser. 2016. "Astrocytic TLR4 at the Crossroads of Inflammation and Seizure Susceptibility." *The Journal of Cell Biology*, 3–5. doi:10.1083/jcb.201611078.

Hunsaker, Michael R. 2012. "Modeling Fragile X Syndrome" 54: 255–69. doi:10.1007/978-3-642-21649-7.

Jacobs, S., C. Cheng, and L. C. Doering. 2016. "Hippocampal Neuronal Subtypes Develop Abnormal Dendritic Arbors in the Presence of Fragile X Astrocytes." *Neuroscience* 324. IBRO: 202–17. doi:10.1016/j.neuroscience.2016.03.011.

Jacobs, Shelley, and Laurie C Doering. 2010. "Neurobiology of Disease Astrocytes Prevent Abnormal Neuronal Development in the Fragile X Mouse" 30 (12): 4508–14. doi:10.1523/JNEUROSCI.5027-09.2010.

Jin, Peng, and Stephen T Warren. 2000. "Understanding the Molecular Basis of Fragile X Syndrome." *Human Molecular Genetics* 9 (6): 901–8.

Joester, Angret, and Andreas Faissner. 1999. "Evidence for Combinatorial Variability of Tenascin-C Isoforms and Developmental Regulation in the Mouse Central Nervous System." *Journal of Biological Chemistry* 274 (24): 17144–51. doi:10.1074/jbc.274.24.17144.

Jones, Emma V., and David S. Bouvier. 2014. "Astrocyte-Secreted Matricellular Proteins in CNS Remodelling during Development and Disease." *Neural Plasticity* 2014. doi:10.1155/2014/321209.

Lee, Seung-hee, Jaehoon Shim, and Bong-kiun Kaang. 2013. "The Role of Cell Adhesion Molecules (CAMs) in Defining Synapse-Specific Function and Plasticity." *Animal Cells and Systems* 17 (1): 1–6. doi:10.1080/19768354.2013.769898.

Lloyd, Peter, and Frederick Scheetz Jones. 2000. "Tenascin-C in Development and Disease : Gene Regulation and Cell Function." *Matrix Biology* 19: 581–96.

Maqbool, Azhar, Emma J Spary, Iain W Manfield, Michaela Ruhmann, Lorena Zuliani-Alvarez, Filomena O Gamboa-Esteves, Karen E Porter, Mark J Drinkhill, Kim S Midwood, and Neil A Turner. 2016. "Tenascin C Upregulates Interleukin-6 Expression in Human Cardiac Myofibroblasts *via* Toll-like Receptor 4." *World Journal of Cardiology* 8 (5): 340. doi:10.4330/wjc.v8.i5.340.

Matsunaga, Naoko, Noboru Tsuchimori, Tatsumi Matsumoto, and Masayuki Ii. 2011. "TAK-242 (Resatorvid), a Small-Molecule Inhibitor of Toll-Like Receptor (TLR) 4 Signaling , Binds Selectively to TLR4 and Interferes with Interactions between TLR4 and Its Adaptor" 242: 34–41. doi:10.1124/mol.110.068064.

McGeachie, Andrew B, Lorenzo A Cingolani, and Yukiko Goda. 2011. "A Stabilising Influence : Integrins in Regulation of Synaptic Plasticity." *Neuroscience Research* 70 (1): 24–29. doi:10.1016/j.neures.2011.02.006.A.

Meiners, S, M L Mercado, M S Nur-e-Kamal, and H M Geller. 1999. "Tenascin-C Contains Domains That Independently Regulate Neurite Outgrowth and Neurite Guidance." *The Journal of Neuroscience : The Official Journal of the Society for Neuroscience* 19 (19): 8443–53.

Midwood, Kim, Sandra Sacre, Anna M Piccinini, Julia Inglis, Annette Trebaul, Emma Chan, Stefan Drexler, et al. 2009. "Tenascin-C Is an Endogenous Activator of Toll-like Receptor 4 That Is Essential for Maintaining Inflammation in Arthritic Joint Disease." *Nature Medicine* 15 (7): 774–80. doi:10.1038/nm.1987.

Molofsk, Anna V., Robert Krenick, Erik Ullian, Hui Hsin Tsai, Benjamin Deneen, William D. Richardson, Ben A. Barres, and David H. Rowitch. 2012. "Astrocytes and Disease: A Neurodevelopmental Perspective." *Genes and Development* 26 (9): 891–907. doi:10.1101 /gad.188326.112.

Pacey, Laura K K, Sihui Guan, Sujeenthar Tharmalingam, Christian Thomsen, and David R. Hampson. 2015. "Persistent Astrocyte Activation in the Fragile X Mouse Cerebellum." *Brain and Behavior* 5 (10): 1–12. doi:10.1002/brb3.400.

Pfeiffer, Brad E, and Kimberly M Huber. 2009. "The State of Synapses in Fragile X Syndrome." *Neuroscientist* 15 (5): 549–67. doi:10.1177/1073858409333075.

Rigato, Franck, Jeremy Garwood, Nicolas Heck, and Catherine Faivre-Sarrailh. 2002. "Tenascin-C Promotes Neurite Outgrowth of Embryonic Hippocampal Neurons through the Alternatively Spliced Fibronectin Type III BD Domains via Activation of the Cell Adhesion Molecule F3 / Contactin Orientation." *The Journal of Neuroscience* 22 (15): 6596–6609.

Samavati, Lobelia, Ruchi Rastogi, Wenjin Du, Maik Hüttemann, Alemu Fite, and Luigi Franchi. 2009. "STAT3 Tyrosine Phosphorylation Is Critical for Interleukin 1 Beta and Interleukin-6 Production in Response to Lipopolysaccharide and Live Bacteria." *Molecular Immunology* 46: 1867–77. doi:10.1016/j.molimm.2009.02.018.

Shen, Yi, Huaping Qin, Juan Chen, Lingyan Mou, Yang He, Yixiu Yan, Hang Zhou, et al. 2016. "Postnatal Activation of TLR4 in Astrocytes Promotes Excitatory Synaptogenesis in Hippocampal Neurons." *The Journal of Cell Biology* 215 (5). doi:10.1083/jcb.201605046.

Stamenkovic, Vera, Stefan Stamenkovic, Tomasz Jaworski, Maciej Gawlak, Milos Jovanovic, Igor Jakovcevski, Grzegorz M. Wilczynski, et al. 2016. "The Extracellular Matrix Glycoprotein Tenascin-C and Matrix Metalloproteinases Modify Cerebellar Structural Plasticity by Exposure to an Enriched Environment." *Brain Structure and Function*. Springer Berlin Heidelberg, 1–23. doi:10.1007/s00429-016-1224-y.

Tancredi, Virginia, Margherita D Antuono, Carla Cafe, Silvia Giovedı, Maria Cristina

Bue, Giovanna D Arcangelo, Franco Onofri, and Fabio Benfenati. 2000. "The Inhibitory Effects of Interleukin-6 on Synaptic Plasticity in the Rat Hippocampus Are Associated with an Inhibition of Mitogen-Activated Protein Kinase ERK." *Journal of Neurchemistry* 75 (2): 634–43.

Trotta, Teresa, Chiara Porro, Rosa Calvello, and Maria Antonietta Panaro. 2014. "Biological Role of Toll-like Receptor-4 in the Brain." *Journal of Neuroimmunology* 268 (1–2). Elsevier B.V.: 1–12. doi:10.1016/j.jneuroim.2014.01.014.

Udalova, A, Kim S Midwood Fui G Goh, Anna M Piccinini, Thomas Krausgruber, Fui G Goh, Irina A Udalova, and Kim S Midwood. 2016. "Novel Autocrine Loop in Inflammation Endogenous Danger Signal Tenascin-C: A Transcriptional Regulation of the Transcriptional Regulation of the Endogenous Danger Signal Tenascin-C: A Novel Autocrine Loop in Inflammation." *The Journal of Immunology at Nagoya City University on The Journal of Immunology* 184: 2655–62. doi:10.4049/jimmunol.0903359.

Udalova, I A, M Ruhmann, S J P Thomson, and K S Midwood. 2011. "Expression and Immune Function of Tenascin-C." *Critical Reviews in Immunology* 31 (2): 115–45. http://www.scopus.com/inward/record.url?eid=2-s2.0-79955665706&partnerID=40&md5=f3c066e282cc3c2652c6f3d57bbdd02e.

Vereyken, Elly J F, Hilda Bajova, Stephine Chow, Pierre N E De Graan, and Donna L Gruol. 2007. "Chronic Interleukin-6 Alters the Level of Synaptic Proteins in Hippocampus in Culture and in Vivo." *Eur J Neurosci* 25 (January): 3605–16. doi:10.1111/j.1460-9568.2007.05615.x.

Wallingford, Jessica, Angela L Scott, Kelly Rodrigues, and Laurie C Doering. 2017. "Altered Developmental Expression of the Astrocyte-Secreted Factors Hevin and SPARC in the Fragile X Mouse Model" 10 (August): 1–12. doi:10.3389/fnmol.2017.00268.

Wang, Gordon X., Stephen J. Smith, and Phillippe Mourrain. 2014. "Fmr1 KO and Fenobam Treatment Differentially Impact Distinct Synapse Populations of Mouse Neocortex." *Neuron* 84 (6): 1273–86. doi:10.1016/j.neuron.2014.11.016.

Wang, Houping, Li Ku, Donna J Osterhout, Wen Li, Amir Ahmadian, and Zhe Liang. 2004. "Developmentally-Programmed FMRP Expression in Oligodendrocytes : A Potential Role of FMRP in Regulating Translation in Oligodendroglia Progenitors." *Human Molecular Genetics* 13 (1): 79–89. doi:10.1093/hmg/ddh009.

Wei, H., I. Alberts, and X. Li. 2013. "Brain IL-6 and Autism." *Neuroscience* 252: 320–25. doi:10.1016/j.neuroscience.2013.08.025.

Wei, Hongen, Kathryn K. Chadman, Daniel P. McCloskey, Ashfaq M. Sheikh, Mazhar Malik, W. Ted Brown, and Xiaohong Li. 2012. "Brain IL-6 Elevation Causes Neuronal Circuitry Imbalances and Mediates Autism-like Behaviors." *Biochimica et Biophysica Acta - Molecular Basis of Disease* 1822 (6). Elsevier B.V.: 831–42. doi:10.1016/j.bbadis.2012.01.011.

Wei, Hongen, Hua Zou, Ashfaq M Sheikh, Mazhar Malik, Carl Dobkin, W Ted Brown, and Xiaohong Li. 2011. "IL-6 Is Increased in the Cerebellum of Autistic Brain and Alters Neural Cell Adhesion, Migration and Synaptic Formation." *Journal of Neuroinflammation* 8 (1). BioMed Central Ltd: 52. doi:10.1186/1742-2094-8-52.

Willis, Cory M, and Stephen J Crocker. 2016. "The Mosaic of Extracellular Matrix in the Central Nervous System as a Determinant of Glial Heterogeneity." *Composition and Function of the Extracellular Matrix in the Human Body*. doi:10.5772/62706.

Yang, Tao, Huan Zhao, Changbo Lu, Xiaoyu Li, Yingli Xie, Hao Fu, and Hui Xu. 2016. "Synaptic Plasticity, a Prominent Contributor to the Anxiety in Fragile X Syndrome." *Neural Plasticity*. Hindawi Publishing Corporation, 1–12. doi:10.1155/2016/9353929.

Yuskaitis, Christopher J, Eleonore Beurel, and Richard S Jope. 2011. "Evidence of Reactive Astrocytes but Not Peripheral Immune System Activation in a Mouse Model of Fragile X Syndrome." *Biochim Biophys Acta* 1802 (11): 1006–12. doi:10.1016/j.bbadis.2010.06.015.Evidence.

Zacharias, Ute, Ursel Norenberng, and Fritz G. Rathjen. 1999. "Functional Interactions of the Immunoglobulin Superfamily Member F11 Are Differentially Regulated by the Extracellular Matrix Proteins Tenascin-R and Tenascin-C * Ute Zacharias ‡, Ursel No." *The Journal of Biological Chemistry* 274 (34): 24357–65.